

**UNCLASSIFIED**

---

---

**AD 261 772**

*Reproduced  
by the*

**ARMED SERVICES TECHNICAL INFORMATION AGENCY  
ARLINGTON HALL STATION  
ARLINGTON 12, VIRGINIA**



---

---

**UNCLASSIFIED**

**NOTICE:** When government or other drawings, specifications or other data are used for any purpose other than in connection with a definitely related government procurement operation, the U. S. Government thereby incurs no responsibility, nor any obligation whatsoever; and the fact that the Government may have formulated, furnished, or in any way supplied the said drawings, specifications, or other data is not to be regarded by implication or otherwise as in any manner licensing the holder or any other person or corporation, or conveying any rights or permission to manufacture, use or sell any patented invention that may in any way be related thereto.

# TECHNICAL DOCUMENTS LIAISON OFFICE UNEDITED ROUGH DRAFT TRANSLATION

261 772

FILE COPY

SPECIAL STEELS AND ALLOYS - COLLECTION OF WORKS, NO. 17  
(Selected Articles)

BY: Various Authors

English Pages: 103



MCL - 711

Reproducible Master is attached for your use in accordance with provisions outlined by Mr. Chapman. Please return as soon as possible to:

Foreign Technology Division  
Technical Library Branch  
(TD-Bla - Mrs. Moots)  
Wright Patterson Air Force Base, Ohio

ASTIA  
AUG 23 1961  
RECEIVED  
TIPDR A

261772

61-4-3  
XEROX

<p>THIS TRANSLATION HAS BEEN PREPARED IN THIS MANNER TO PROVIDE THE REQUESTER/USER WITH INFORMATION IN THE SHORTEST POSSIBLE TIME. FURTHER EDITING WILL NOT BE ACCOMPLISHED BY THE PREPARING AGENCY UNLESS FULLY JUSTIFIED IN WRITING TO THE CHIEF, TECHNICAL DOCUMENTS LIAISON OFFICE, MCLTD, WP-AFB, OHIO</p>	<p>PREPARED BY: TECHNICAL DOCUMENTS LIAISON OFFICE MCLTD WP-AFB, OHIO</p>
---	---

VARIOUS AUTHORS

SPETSIAL'NYE STALI I SPLAVI  
SBORNIK TRUDOV  
NO. 17

Publishing Office

State Scientific and Technical Publishing Office for Literature  
on Ferrous and Nonferrous Metallurgy  
Moscow, 1960

Foreign Pages: 327-357  
398-418  
472-488

PROPERTIES AND PECULIARITIES OF SPECIAL ALLOYS WITH  
HIGH NICKEL AND MOLYBDENUM CONTENT

by

Yu.M.Chizhikov, Candidate in Technical Sciences

Special alloys with high nickel and molybdenum content are used in <sup>the</sup> chemical industry. The best known of these are <sup>the</sup> alloys A (NM20, EI460), B (NM30, EI461) and Ts (NM17Kh15V5). Table 1 gives their approximate chemical composition.

Table 1

Approximate Chemical Composition of High-Nickel-Molybdenum Alloys, %

Alloy

A

B

Ts

These alloys have a number of important properties. First of all, exceptionally high resistance to various aggressive media at high temperatures and pressures. Their technological properties make their production very

the  
 difficult. This Article gives <sup>A</sup> experimental data ~~that have been~~ accumulated  
 in the industrial development ~~of the production~~ of these alloys\*.

### Corrosional Properties of the Alloys

Alloys NM20, NM30, NM17Kh15V5 have high anticorrosional <sup>or</sup> properties in various chemically active media.

Alloy NM20 has good chemical resistance to nonoxidizing acids such as ~~HCl~~ <sup>hydrochloric</sup> and ~~sulfuric acid (dilute)~~ <sup>and dilute H<sub>2</sub>SO<sub>4</sub></sup>. It resists the action of HCl and H<sub>2</sub>SO<sub>4</sub> of any concentration at temperatures ~~up to~~ up to 70°C. At acid concentrations under 50% it is suitable for use at the boiling points of the acid.

Alloy NM30 has high chemical resistance <sup>to</sup> boiling HCl and H<sub>2</sub>SO<sub>4</sub> at any concentration, in ~~moist H<sub>2</sub>S gas etc.~~ <sup>hydrofluoric acid, moist hydrogen chloride, etc.</sup>

Alloy NM17Kh15V5 ~~resists~~ resists corrosion under the action of powerful oxidizing ~~agents~~ agents, such as moist ~~chlorine gas~~ chlorine gas, nitric acid, sulfuric acid, etc.

Alloy B (NM30) has the best resistance; in the heat-treated condition, its rate of corrosion even in boiling acid does not exceed 0.04 mm/year.

### Physical Properties

The physical properties of alloys A, B and Ts are given in Table 2.

\* Engineer M.L.Zaytsev, Engineer A.N.Funde and Technician A.A.Mishin participated in this work.

Table 2

Physical Properties of Alloys Hast<sup>e</sup> Alloy A, B and Ts

(According to Data of Metals Handbook, 1948)

Properties	Alloy A	Alloy B	Alloy Ts
Specific gravity, gm/cm <sup>3</sup>	8.80		
<b>Melting</b> point (solidus and liquidus), °C			
Specific heat, cal/gm, °C			
Thermal conductivity at 25°C, cal/sec °C			
Resistivity at 25°C, per cm, microohms			
Mean coefficient of thermal expansion per <del>100</del> degree C.			
from 0 to 100°C			
from 0 to 1000°C			

Mechanical Properties

As will be seen from Table 3, all three alloys possess high strength.

Figure 1 shows the variation of their mechanical properties with temperature.

Figure 2 shows the variation of the mechanical properties and hardness of alloys A, B and Ts with ~~relative upset~~ <sup>reduction</sup> in cold-rolling. Before cold-rolling all the specimens were given a softening heat treatment (heating to 1180 - 1200°C, <sup>quenching</sup> ~~cooling~~ in water or air).

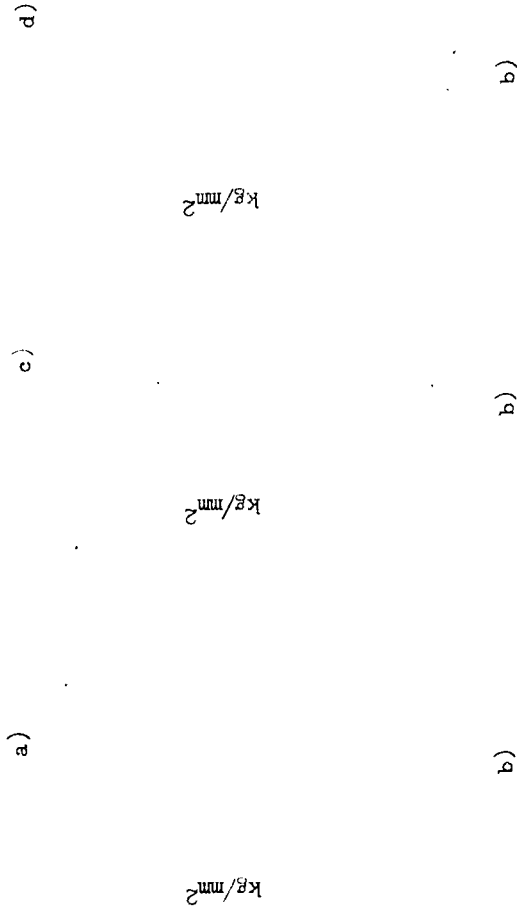


Fig.1 - Temperature Dependence of Tensile Strength  $\sigma_T$ , Yield Point  $\sigma_Y$  and Proportional Limit  $\sigma_P$  of Alloys A, B and C

Specimens hot-rolled and heat-treated 2 hrs at 1180°C, then cooled in water

a) Alloy A; b) Test temperature, °C; c) Alloy B; d) Alloy C

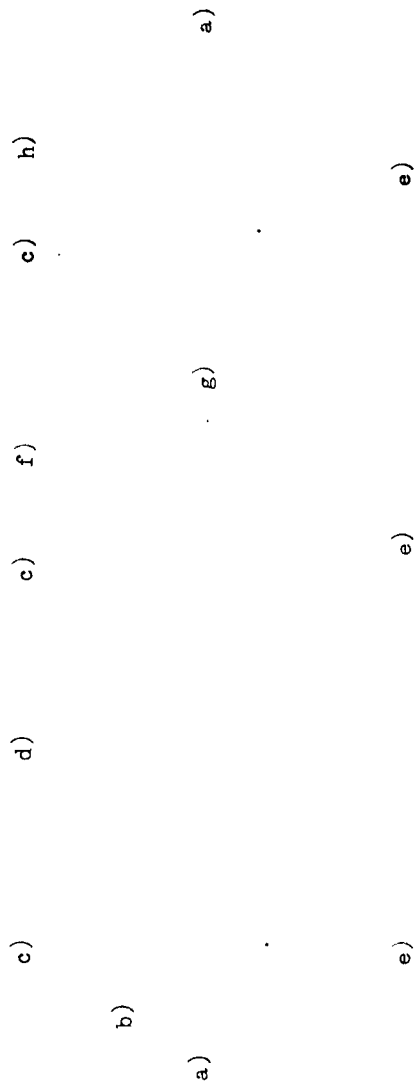


Fig.2 - Relation between Mechanical Properties of Alloys A, B and Ts and

Reduction,  $\frac{H-h}{H} \cdot 100\%$ , in Cold-Rolling

- a)  $\sigma_p$  Elongation  $\epsilon$ , %; reduction  $N$ , %; b)  $\sigma_p$  strength,  $\sigma_p$ , kg/mm<sup>2</sup>; c) Alloy A; d) Reduction, %; e) Alloy B; f) Hardness, Hv; g) Alloy Ts

Table 3

Mechanical Properties of Alloys at Room Temperature  
(Sheet, Heat-Treated)

Alloy	Heat	Tensile Strength, kg/mm <sup>2</sup>	Yield Strength, kg/mm <sup>2</sup>	Proportional Limit, kg/mm <sup>2</sup>	Elastic Limit, kg/mm <sup>2</sup>	Reduction <del>in Area</del> %	Elongation, %
NM20 (A)	--						
NM30 (B)	37B						
NM30 (B)	143C						
NM17Kh15V5	22Ts						
NM17Kh15V5	23Ts						
NM17Kh15V5	24Ts						

Structure of the Alloys

Alloys A and B consist mainly of a solid solution of molybdenum and iron and nickel. On cooling from high temperatures, intermetallic compounds of variable composition of the iron molybdenite type ( $Fe_3Mo_2$ ) and nickel molybdenite type ( $MoNi$ ) are segregated. At sufficiently high carbon concentration, the solution also contains double carbides of iron and molybdenum. ~~XXXXXXXXXX~~ In presence of an excess of silicon, silicides are formed in the alloys. The iron molybdenite partially passes into solid solution on heating; the nickel molybdenite does not pass over into solid solution at any temperature. No intermetallides are observed under the microscope in these alloys. Their presence may be judged from the variation of the hardness of the metal on heating to various temperatures, followed by cooling in water.

Best Available Copy

Figures 3 and 4 show the microstructures of alloys A and B. The microstructures are of interest because they explain certain features of the alloys in hot-working.

Considering the microstructure of alloy A (Fig.3) it will be seen that new equiaxed grains appear at 1200°C. On reduction of 15%, the instant indicating the formations of new recrystallized grains along the old grain boundaries is fixed. At 1050°C (at both reductions), the as-cast structure persists to a considerable extent. On 60% reduction, a fibrous structure recalling that of cold-rolled steel is distinctly visible. All this indicates that the temperature of 1050°C is not a temperature at which the process of recrystallization normally takes place for alloy A.

picture with still

An analogous ~~XXXXXXXXXXXXXXXX~~ greater contrast is obtained in alloy B

332

(Fig.4). At 1050°C. <sup>at</sup> with both ~~re~~ductions, no new grains were formed. Comparing the microstructure ~~to~~ corresponding to the temperature 1050°C with the microstructure of the same alloy in the as-cast condition (Fig.5), one may convince oneself that rolling at this temperature leads only to <sup>refinement</sup> ~~combination~~ of the as-cast structure, to giving it an oriented and fibrous form, with ~~the~~ a degree of fiber formation increasing with the degree of reduction. At 1050°C, obviously,

a

c

b

d

Fig.3 - Microstructure of Rolled Alloy A. 100 x:

a - 15% reduction at 1050°C; b - 15% reduction at 1200°C;

c - 60% reduction at 1050°C; d - 60% reduction at 1200°C

the process of recrystallization does not yet take place during deformation.

It is only possible ~~that~~, at this temperature, <sup>relief</sup> ~~the removal~~ of part of the stresses arising during deformation does take place. At 1200°C, at all reductions, the process of recrystallization does take place with formation of new equiaxed grains.

Best Available Copy

Heating to higher temperatures leads to substantial changes along the grain boundaries. This is clearly visible in the microstructure of alloy MM20 (Fig.6) heated to 1250 and 1280°C. At 1280°C, melting and formation of a

a

b

c

d

Fig.4 - Microstructure of Rolled Alloy B. 100 x  
 a - 15% reduction at 1050°C; b - 15% reduction at 1200°C;  
 c - 60% reduction at 1050°C; d - 60% reduction at 1200°C

Fig.5 - Microstructure of Steel E in the As-Cast Condition

334

liquid phase took place along the grain boundaries. This phase again solidified after cooling.

~~As~~  
\* As in text.  
Translata

a

b

Fig.6 - Microstructure of Alloy NM20:

a - Heated to 1250°C. 100 x; b - Heated to 1280°C. 300 x

At 1250°C, melting is also observed, but not along all the grain boundaries.

The same picture is observed in alloy NM30. The possibility of this phenomenon

does not require <sup>special</sup> ~~no particular~~ explanation, since the melting point of alloy A

is 1300 - 1330°C, and that of alloy B 1320 - 1350°C.

Analysis of the microstructure of these alloys shows them to possess a very narrow range of hot-deformation temperatures. The danger of overheating the metal at temperatures over 1200°C (the length of heating and the furnace atmosphere are very important here) and the high recrystallization temperature (over 1000 - 1050°C) are responsible for the technological properties of the alloys and their forgeability, which will be discussed below.

f)

e)

c)

a)

b)

d)

d)

d)

Figs. 1 - Temperature Dependence of Elongation and Reduction ~~in Area~~ <sup>in Area</sup> of Specimens of Alloys B and Ts. The specimens of these alloys were hot-rolled and heat-treated 2 hr at 1220°C, then ~~checked~~ <sup>checked</sup> in water

- a) Elongation  $\delta$ , %; b) Reduction ~~in Area~~ <sup>in Area</sup>, %; c) Alloy B; d) Test temperature, °C; e) Alloy Ts; f) Alloy Ts, cast

### Plasticity of the Alloys

The plasticity of these three alloys may be judged from the values of the elongation and reduction ~~in area~~ <sup>in area</sup> of the specimens during the tensile test and from the results of a study of the impact strength and wedge ~~lowering~~ <sup>rolling</sup>.

Figure 7 gives the curves of temperature variation of the elongation and reduction in area for alloys B and Ts. These alloys have maximum plasticity around 1100°C.

The variation of the plastic properties with temperature from the impact strength is shown in Fig. 8. The impact strength is minimum at around 1000°C. The high plastic properties correspond to temperatures of 1100 and 1200°C.

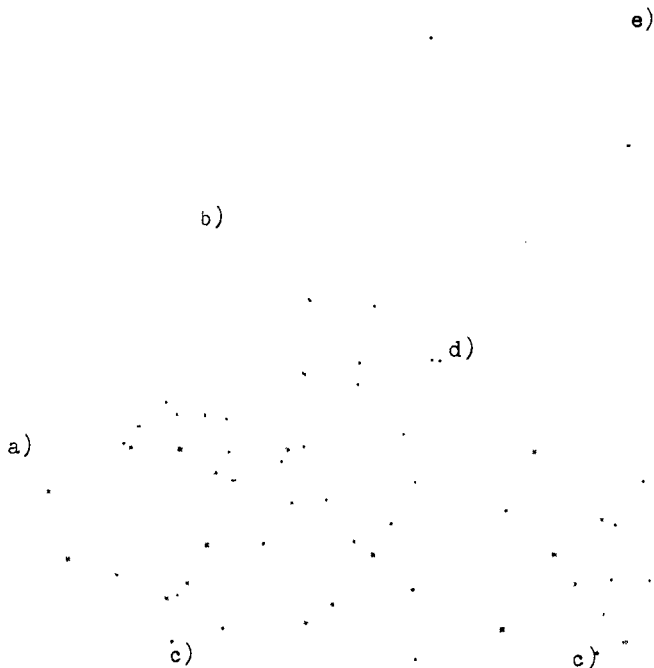


Fig.8 - Temperature Dependence of Impact Strength of Alloys B and Ts

Alloy B: ~~treated 2 hr at~~ 1160-1180°C, then cooled in water.

Alloy Ts; specimens 1, 2 - Forged and heat-treated 2 hr at 1210°C, *quenched* cooled in water; Specimens 3, 4 - Cast without heat treatment;

Curves 1, 3 and 4 - Heated to test temperature; Curve 2 - Cooled in furnace ~~XX~~ from 1210°C to test temperature

a) Impact strength, kg/cm<sup>2</sup>; b) Alloy B; c) Test temperature °C;

d) Impact strength  $\propto K$ , kg/cm<sup>2</sup>; e) Alloy Ts

337

From the condition of the side edges of specimens of alloys rolled to various reductions, it will be seen that the plasticity of alloy B at 1050°C is lower than at 1200°C (Fig.9). This follows from the fact that at the lower temperature tears were formed on the edges at a reduction as low as 32.5%.

while at 1200°C their formation commenced at reduction 50.9%.

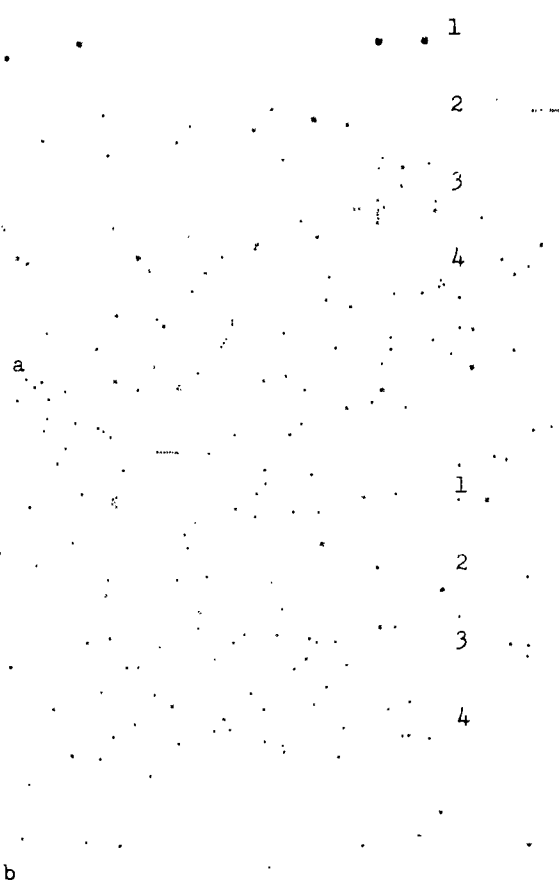


Fig.9 - External View of Specimens of Alloy B Rolled to Various Reductions:

a - At 1050°C with reductions: 1 - 32%; 2 - 21.0%; 3 - 15.7%; 4 - 9.6%;

b - At 1200°C with reductions: 1 - 50.9%; 2 - 30.5%; 3 - 19.5%;

4 - 12.6%

Figure 10 shows cast specimens of alloy A rolled to a wedge. It will be seen here that at 1200°C small tears begin to form at reductions over 40%.

These data show all three alloys to possess relatively low plasticity.

The temperature range of their deformation is narrow, and is of the order of 1050 - 1220°C.

H-h mm  
 $\frac{H-h}{H} \times 100\%$

H-h mm  
 $\frac{H-h}{H} \times 100\%$

H-h mm  
 $\frac{H-h}{H} \times 100\%$

Fig.10 - Appearance of Specimens of Cast Alloy A after  
 Wedge Rolling at Various Temperatures:

a - 1100°C; b - 1200°C; c - 1280°C



Fig.11 - Variation of Hardness of Binary Nickel-Molybdenum Alloys with Molybdenum Content and Temperature  
(Cooling in Water)

a) Hardness,  $H_v$ ; b) Temperature,  $^{\circ}C$

as indicated by the peaks on the curves (Fig.11). The variation in the properties with increasing molybdenum content is due to the segregation of an excess phase (apparently nickel molybdenite), which is readily detected from the changes in the microstructure as well (Fig.12).

The alloying elements have a great influence on the plastic properties of these alloys. The influence of molybdenum on ~~XXXX~~ forgeability has been established for binary nickel-molybdenum alloys. It was found that the forgeability (plasticity) of these alloys declines with increasing molybdenum content; at less than 20% Mo the alloys have good forgeability; at about 40% they become brittle and unforgeable. With increasing molybdenum content their hardness increases. At over 20% Mo the alloys are dispersion hardening

a

b

c

Fig.12 - Change in Microstructure of Binary Nickel-Molybdenum Alloys with their Molybdenum Content, %:

a - 22.8, 150 x; b - 44.2, 150 x; c - 44.2, 650 x

Silicon has an exceptionally great influence on the properties of high-nickel-molybdenum alloys. Table 4 gives data on alloy NM30 of the following chemical composition: 0.04% C, 0.88% Mn, 64.5% Ni, 30.0% Mo, 4.59% Fe.

Table 4

## Variation in Hardness of Alloy B with its Silicon Content

Ingot No.	Silicon Content, %	Hardness of Ingots after Pouring and Cooling, $H_V$	Hardness of Forgings after Forging and Air Cooling, $H_V$ <i>Amersham</i>	Hardness of Forgings after Heat Treatment: 1130°C, 10 min; Water, $H_V$
1				
2				
3				
4				

As found on forging that only ingots 1 and 2 were forged without defects. At high silicon content the forgeability of the ingots ~~was~~ <sup>declined,</sup> ~~was~~ and tears appeared on the forgings, and their resistance to deformation was appreciably increased. Ingot 5 had the poorest forgeability. A similar behavior of the metal was observed in hot-rolling. Strips from ingots 1 and 2 were rolled without the formation of cracks and tears on the longitudinal edges. Cracks and tears were, however, formed on the edges of the strip from ingots 3, 4 and 5, most of all from ingots 4 and 5 (Fig.13).

The hot-rolled strip so obtained, 2.5 mm thick, after heat treatment (heating 30 min to 1190°C, and <sup>quenching</sup> cooling in air) ~~was~~ <sup>was</sup> rolled on a <sup>four-high</sup> ~~quench~~ rolling mill with rolls 180 mm in diameter. The strip from ingots 1, 2 and 3 ~~was~~ <sup>was</sup> rolled

intermediate working without ~~XXXXXXXXXXXXXXXXXXXX~~ to thickness <sup>of</sup> 0.5 mm, with a total reduction of about 90%. At 30% total reduction, small tracks began to appear on the edges of the strip from ingot 3. The strip from ingot 4 *cracked* along the edges at the first reduction; and the strip from ingot 5 broke at the very first reduction (Fig.14).

Thus silicon in alloy NM30 at the same time lowers the plasticity of the metal and increases the resistance to deformation. This effect on the properties of the alloys may be explained by the formation of a new phase in the form of silicides (probably  $MoSi_2$ ?) which is plainly visible on Figs.15 a, b, c, d, e. At low silicon content <sup>there is</sup> a very little of the new phase, but with increasing silicon there is more and more of it; it is located both along the grain boundaries and in the grain interiors. In spite of the fact that the

1

2

3

4

5

Fig.13 - Appearance of Specimens of Alloy with Varying  
Silicon Content after Hot-Rolling. Si content in alloys.

1 - 1.3%; 2 - 0.98%; 3 - 0.59%; 4 - 0.23%; 5 - 0.056%

(the strip edges are on top)

1

2

3

a) b) c)

5

4

Fig.14 - Appearance of Specimens of Alloy with Various Silicon Contents  
after Cold Rolling

a) Strip No.; b) Silicon content, %; c) Total reduction, %



Fig.15 - Microstructure of Alloy NM30 with Varying  
Content of Silicon, %. 100  $\times$   
a - 0.056; b - 0.23; c - 0.59; d - 0.98; e - 1.3

alloys were all heated to the same temperature, which ~~was~~<sup>was</sup> sufficiently high, 1150°C, the grain size at higher silicon contents was considerably smaller than at low<sup>Si</sup> content. This indicates that the silicides retard the grain growth of the metal during its recrystallization, ultimately leading to a lowering of the plastic properties of the alloy and to an increase in its resistance to deformation.

On the basis of the data obtained, the conclusion must be drawn that the silicon content in these alloys should be as low as possible, and must not exceed 0.3 - 0.4%.

#### Resistance of Alloys to Deformation during Rolling

A study of the resistance to deformation was made by measuring the pressure of the metal on the roll by the aid of capacitance measuring instruments during rolling of specimens 20 mm and 12 mm thick ( $H = \text{const}$ ), and 40 mm wide on a 400-mm rolling mill at a ~~rate~~<sup>speed</sup> of 1.0 m/sec. The specimens  $H = 20$  mm were rolled at 1050 - 1250°C; the specimens  $H = 12$  mm at 20, 200, 400, 600, 1050 - 1250°C. Each specimen was rolled in a single pass at various reductions. The specimens were heated in tubular guffles in a gas chamber furnace. To obtain comparative data, <sup>similar</sup> specimens ~~of the same kind~~ of steel 1 were rolled besides specimens of alloys NM20 (A), NM30 (B) and NM17Kh15V5 (Ts).

Figure 16, a, b, c shows the curves of the dependence of the resistance <sup>to deformation</sup> of alloys A, B and Ts to deformation when rolled at  $H = \text{const} = 12$  mm.

It will be seen that at all temperatures and reductions the resistance

of alloys A, B, and Ts to deformation is considerably higher than that of St.1 under comparable conditions. The resistance of these alloys to deformation is almost 5 - 6 times as great for these alloys as for St.1 at 1160°C and 25% reduction, and 4 - 5 times as great at 1000°C. Alloy B has a higher resistance to deformation than alloy A. This difference is the greater, the lower the rolling temperature.

The rolling temperature has a strong effect on the resistance of both alloys to deformation. In the temperature range from 600 to 1000°C, the resistance of both alloys to deformation decreases very slightly, but in a narrow interval (from 1000 to 1050°C) it falls very sharply, and then remains almost constant up to about 1120°C, and finally falls sharply again. For steel St.1 the decrease in resistance to deformation ~~proceeds along~~ <sup>follows</sup> a smooth concave curve, more intensely from 600 to 1000°C than at temperatures over 1000°C (Fig.17).

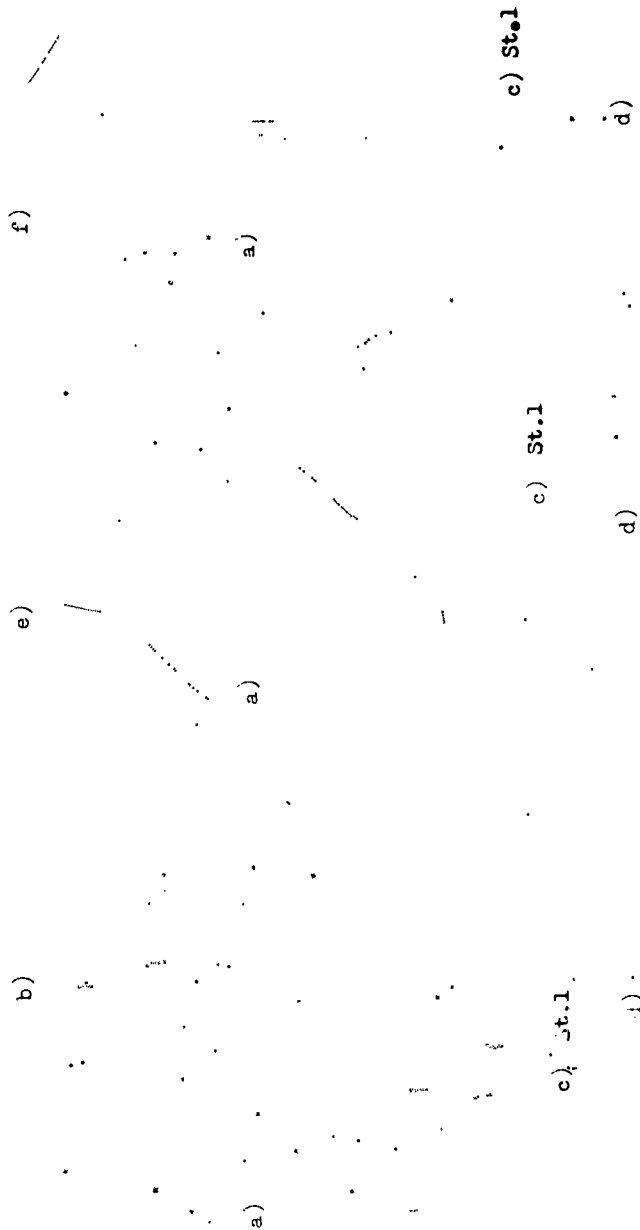


Fig. 16 - Relation between resistance of Alloys A, B and Ts to Deformation and the Reduction in Hot Rolling ( $n = \text{const} = 12 \text{ mm}$ )

a) Resistance to deformation,  $\text{kg/mm}^2$ ; b) Alloy A; c) Steel St.1; d) Reduction,  $\frac{H-h}{H} \cdot 100, \%$

e) Alloy B; f) Alloy Ts

EU461.30  
EU460.30  
EI461  
EI460  
St.1

a)

b)

EU461.30  
EU460.30

EI461.8

EI460.10

St.1.30

St.1.10

a)

b)

EI461

EI460

St.1

a)

b)

Fig.17 - Effect of Rolling Temperature on Resistance of Alloys to Deformation

1, 2, 3 -  $H = 12$  mm; 4, 5 -  $H = 20$  mm

at 20% Reduction

a) Resistance to deformation,  $\text{kg}/\text{mm}^2$ ;

b) Rolling temperature,  $^{\circ}\text{C}$

Fig.18 - Effect of Speed Rolling on Resistance of Alloys to Deformation ( $\delta = 370$  mm,  $t = 1100^{\circ}\text{C}$ ); the Figures in the Curves Show the Reduction, %

a) Resistance to deformation,  $\text{kg}/\text{cm}^2$ ;

b) Rolling speed,  $\text{m}/\text{sec}$

Fig.19 - Relation between Resistance of Alloys to Deformation and the Reduction in Cold Rolling

a) Resistance to deformation,  $\text{kg}/\text{mm}^2$ ;

b) Reduction, %

c) Alloy Ts

Figure 18 shows the variation of the resistance of both alloys to deformation with increasing rolling rate, which is of great interest.

The relation between the resistance of all three alloys to deformation and the reduction in cold rolling is shown in Fig.19. The cold rolling was done on a rolling mill with rolls 432 mm in diameter at 40 rpm; thickness of specimen 4.5 mm; width 40 mm.

#### Widening

The tendency of alloys NM20 and NM30 to widening was studied at  $H = \text{const.}$  Specimens of constant thickness  $H = 20$  mm, 40 mm wide, were rolled on rolls 400 mm in diameter at a rolling speed of 1.0 m/sec. The specimens were heated to various temperatures. For comparison similar specimens of carbon steel (St.1) were also rolled at the same time. The data so obtained are represented in Fig. 20, b in the form of curves of the widening index against the reduction at various rolling temperatures. As will be seen, both alloys have a greater tendency to widening than St.1.

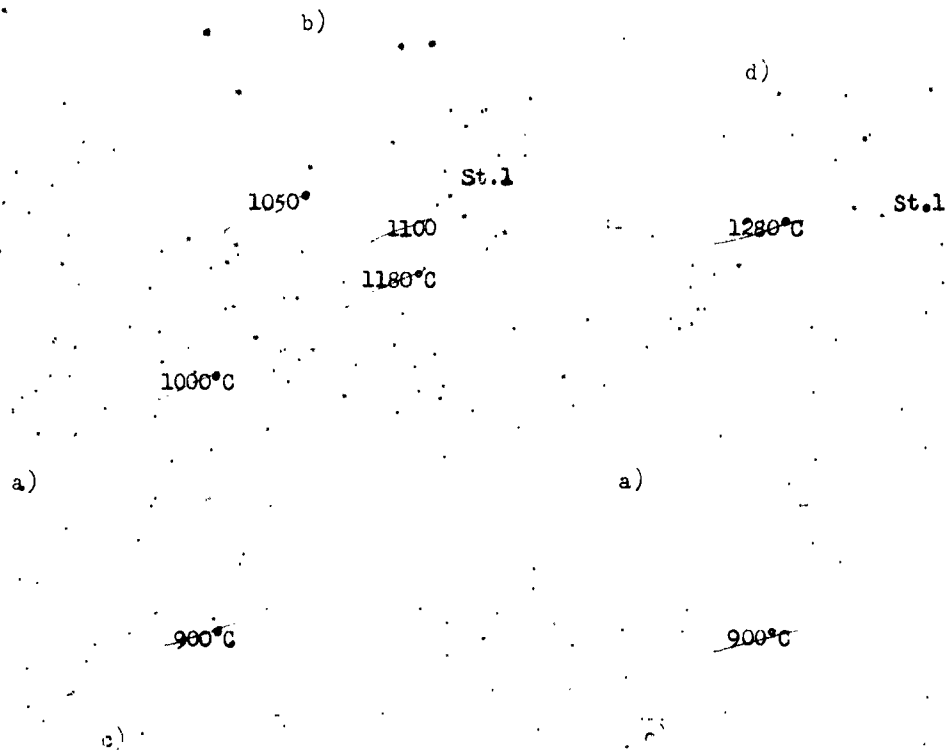


Fig.20 - Relation between Widening Index of Alloys A and B and the Reduction in Rolling at Various Temperatures

a) Widening index,  $\Delta b/\Delta h$ ; b) Alloy A; c) Reduction,  $\frac{H-h}{H} \cdot 100, \%$ ; d) Alloy B;

### Stampability

Stampability in the cold condition was determined by the method of *forming* ~~extrusion~~ on an Ericsson instrument. Figure 21 shows the relation between the stampability of strip of alloys NM30 and NM17Kh15V5 and the thickness of the strip. Before the test all specimens were given a softening heat treatment:



Fig.21 - Relation between Stampability of Strip of Alloys B and Ts and the Thickness of the Strip (Radius of Punch 10 mm):  
 1 - Heat treatment: 5 min at 1180°C, air; 2 - Heat treatment, 5 min at 1180°C, air + cold rolling  $\frac{H-h}{H} = 2.5\%$ ; 3 - Heat treatment 5 min at 1220°C, air  
 a) Stampability, mm; b) Alloy B; c) Thickness of strip, mm;  
 d) Alloy Ts

For alloy Ni30, some of the specimens after heat treatment were cold-rolled to 25% reduction. The experimental data show the stampability of both alloys to depend on the thickness of the strip and the reduction in cold rolling.

THE EFFECT OF BARIUM AND CALCIUM ON THE "LIFE"  
OF NICHROMES

by

Professor M.V.Pridantsev, Doctor of Technical  
Sciences, and Engineer A.V.Merlina

The favorable influence of cerium and barium on the "life" of iron-chromium-aluminum alloy No.2 has been established by the Steel Institute of the Central Research Institute for Ferrous Metallurgy. It has also made a study of the influence of barium and calcium on the "life" of nichrome alloys of grade Kh15N60 and Kh20N80.

Barium and calcium are powerful deoxidizers, promoting the production of a purer alloy with decreased content of oxides along the grain boundaries.

The addition of barium and calcium to nichrome in the alloys is of great interest with respect to the improvement of their heat resistance.

\* "Zhivuchest'", quotation marks in original. This term has been rendered "life" in this translation. It refers apparently to the time at high temperature before onset of a specified increase in resistivity of the material as wire.

It is well known from the works of G.V. Akimov (Bibl.1) that the addition of calcium to nichrome tends to improve the mechanical properties of the alloy at high temperatures and increases the resistance of the grain boundaries to the action of hot gases.

The effect of barium on the properties of nichromes was studied from 0.6 to 1% and that of calcium from 0.2 to 0.6%. Table 1 gives the chemical composition of the alloys investigated. The experimental specimens of the alloys were tested for "life", resistivity, temperature coefficient of resistance, and mechanical properties. The properties of the alloys were studied on wire 0.6 mm in diameter in the heat treated condition.

#### Preparation of the Experimental Alloys

The alloys were melted in a 30 kg high frequency furnace with a basic crucible according to the technology customarily used for nichromes.

The barium was introduced in the form of an aluminum-barium master alloy, the calcium in the form of silicocalcium. The master alloys were added to the molten metal 7 - 8 min before pouring.

Table 1

## Chemical Composition of the Experimental Alloys, %

Grade of Alloy	Heat No.
----------------	----------

## Series of Alloys with Varying Additions of Calcium

Industrial nichrome
------------------------

Kh15N60

Kh20N80

## Series of Alloys with Varying Additions of Barium

Kh15N60

Kh20N80

---

\* The content of Ba and Ca given is the calculated value.

After introduction of the additions the furnace was turned off for 4 - 5 min, and was then turned on again to full power until the metal was poured, in order to give the addition elements time to react completely in the metal.

The barium was determined by the chemical and <sup>spectral</sup> spectroscopic methods; the calcium only by the <sup>spectral</sup> spectroscopic method. In all cases ~~the~~ barium and calcium was not detected in the alloys obtained. Apparently both barium and calcium, when added to the molten metal, perform the functions of a deoxidizer and pass into the slag, and even if they do remain in the metal, it is in such small quantities as to be difficultly determined by the spectral and chemical methods.

The ingots were heated to 1050 - 1100°C for forging. All the ingots forged satisfactorily. During the preparation of the wire, no unfavorable effect of the additions of barium and calcium on the nichromes was noted.

351

#### Mechanical Properties

The mechanical properties (tensile strength and elongation) at normal temperature of the alloys with various additions of barium and calcium, as compared with ordinary nichromes, are given in Table 2.

Table 2

## Mechanical Properties of the Alloys Studied

Grade of Steel	Tensile Strength, kg/mm <sup>2</sup>	Elongation, %
Kh15N60		
Kh15N60 with calculated addition of barium from 0.6 to 1%		
Kh15N60 with calculated addition of calcium from 0.2 to 0.6%		
Kh20N80		
Kh20N80 with calculated addition of barium from 0.6 to 1%		
Kh20N80 with calculated addition of calcium from 0.2 - 0.30%		

It will be seen from these data that in almost all cases the alloys treated with calcium or barium had a tensile strength somewhat higher than that of ordinary nichrome; and the elongation in all cases <sup>was</sup> also higher.

The favorable effect of barium on the long-time strength is very distinct. For example, at 700°C and stress 11 kg/mm<sup>2</sup>, for alloy Kh15N60 without barium, the time to rupture was 48 hr, while the same alloy treated with barium under

the same test conditions showed a time to rupture of 135 - 156 hr.

Thus the treatment of alloy Kh15N60 and Kh20N80 with barium or calcium <sup>led</sup> leads to an improvement of the mechanical properties at normal temperature, and to a considerable improvement of the tensile properties in long-time tests. The presence of barium and calcium was not detected in the finished alloys. The improvement may be attributed to their action as powerful deoxidizers, i.e., to the improved purity of the metal, especially along the grain boundaries.

#### Resistivity and Temperature Coefficient of Resistance

The resistivity was investigated both at normal temperature and on heating, as a function of the calculated additions of barium and calcium. At least six specimens of each heat were tested. Good agreement of the results was noted in all heats.

No distinct dependence of the resistivity on the calculated addition of barium or calcium was noted for Kh15N60 and Kh20N80 at normal temperature; although the difference in the heats studied was measured in hundredths, the addition of barium to nichromes still caused <sup>a certain</sup> ~~an~~ tendency to increased resistivity.

The tests were run in the temperature range 20 - 1150°C. The resistivity increases more sharply in the specimens of alloy Kh15N60, since this is less stable. At higher calculated addition of barium the resistivity ~~increases~~ <sup>throughout</sup> the entire temperature range ~~is~~ <sup>is</sup> higher (Fig.1).

Alloy Kh15N60, with the highest (0.6%) calculated addition of calcium, ~~is~~

<sup>had</sup> heating has a slightly higher resistivity <sup>when heated</sup> than the same alloy without calcium (Fig.2).

The alloys Kh20N80 with additions of barium and calcium <sup>had</sup> have a higher resistivity and ~~consequently~~ a lower temperature coefficient of resistance throughout the entire temperature range (Figs.1,2).

#### "Life" of the Alloys

The tests of the "life" of the alloys were run by the accelerated method on wire 0.6 mm in diameter, pursuant to GOST 2419-44. Alloy Kh15N60 with various additions of barium and calcium was tested at 1100°C, the working temperature of nichrome of grade Kh15N60. Alloy Kh20N80 with various additions of barium and calcium was tested at the working temperature of 1175°C.

Six specimens of each heat were tested. The test of the "life" of the alloys is a combined form of test in which the favorable effect of barium and calcium on the nichromes was displayed.

Figure 3 shows the results of the "life" test on alloys Kh15N60 and Kh20N80 with various additions of barium. It will be seen that nichrome treated with barium has a "life" twice as high as the ordinary alloy. There is no direct dependence of the "life" of the alloy on the calculated addition of barium. Apparently the "life" depends not so much on the quantity of the element added as on the method of its addition to the molten metal. The alloys

a)

b)

a

c)

Fig.1 - Variation of the Resistivity and Temperature Coefficient of Resistance of Alloys Kh15N60 (a) and Kh20N80 (b) with ~~various~~ <sup>various</sup> Additions of Barium.

Calculated Additions of Barium:

1 - Without barium; 2 - 0.6%; 3 - 0.8%; 4 - 1.0%

a) Resistivity, ohms mm<sup>2</sup>/m; b) Temperature coefficients of resistivity,  $\alpha \times 10^{-4}$ ;

c) Heating temperature, °C

a)

b)

a

b

c)

Fig. 2 - Variation of the Resistivity and Temperature Coefficient of Resistance of Alloys

Kh15N60 (a) and Kh20N80 (b) with Various Additions of Calcium on Heating. Calculated

Additions of Calcium:

1 - Without calcium; 2 - 0.2%; 3 - In alloy Kh15N60 - 0.4%; in alloy Kh20N80 - 0.3%; 4 - In alloy Kh15N60 - 0.4%

a) Resistivity, ohms  $\text{mm}^2/\text{m}$ ; b) Temperature coefficients of resistivity,  $\alpha \times 10^{-4}$ ;

c) Heating temperature, °C

a)

a

b

b)

Fig.3 - Variation of Resistance during Test of "Life" of Alloys Kh15N60 (a) at 1100°C and Kh20N80 (b) of 1175°C with Various Additions of Barium:

I - 1.0%; II - 0.8%; III - 0.6%; IV - Without barium

a) Resistance, ohms; b) Time, hr

a)

b)

a)

b)

Fig. 4 - Variation of Resistance during "Life".... Test of Alloys Kh15N60 (a) at 1100°C; and Kh20N80 (b) at 1175°C with ~~Variations~~ Additions of Calcium to Alloy Kh15N60;

I - 0.6%, II - 0.4%, in alloy Kh20N80; III - 0.2%; IV - 0.3%; V - 0.2% VI - Without calcium

a) Resistance, ohms; b) Time, hr

~~is~~ <sup>treated</sup> with barium shows a more stable resistance during the time of the "life" test. Calcium had a still more effective influence on the "life" of nichromes. For example, the "life" of alloy Kh15N60 with the calculated addition of 0.4% Ca increased from 69 hr to 444 hr (Fig.4), i.e., by a factor of six; for alloy Kh20N80 it increased from 58 to 290 hr (Fig.4). The alloys treated with calcium had a still more stable resistance during the "life" test than those treated with barium.

Analysis of the microstructure of the specimens tested for "life" indicates that the process of oxidation of ordinary nichromes proceeds at an accelerated rate along the grain boundaries, while in alloys treated with barium or calcium it proceeds at a retarded rate along those boundaries.

#### Conclusions

1. The ~~additional~~ <sup>supplementary</sup> introduction of barium or calcium <sup>into</sup> nichromes improves their mechanical properties at normal temperature, their heat resistance and their life.
2. The addition of barium (0.6 - 1%) to ohmic resistor alloys of grades Kh15N60 and Kh20N80 improves their "life" by a factor of 2 - 2.5.
3. The addition of calcium to the same alloy is more effective: introduction of 0.2 - 0.6% of calcium improves the "life" of alloys Kh15N60 and Kh20N80 by a factor of 4 - 6.
4. No relation between the "life" of nichromes and the quantity of barium or calcium added was found. Apparently in this case the "life" depends

not so much on the quantity of barium or calcium added as on the time and  
method of their introduction <sup>into</sup> ~~at~~ the molten metal.

3



impact strength that is required for automatic ~~WINDING~~<sup>winding</sup> of the grids. The wire of a vacuum tube must have appropriate physical properties: a high vaporization point, a low coefficient of thermal expansion and a relatively good thermal conductivity for removal of the heat formed in the grid ~~due to the heating~~ of the strongly heated cathode.

Molybdenum wire is used for the grids of most electron tubes. This wire is easily degassed, has high strength at room and elevated temperatures, a high modulus of elasticity, a low temperature coefficient of thermal expansion, and relatively good thermal conductivity. But this metal can be drawn into wire only with difficulty. Molybdenum wire must be drawn in the hot state at low speeds. Before deformation in the heated state, the wire is covered with

*(a colloidal solution of graphite).*

399

aquadag. ~~The~~ aquadag must then, under all circumstances, be cleaned off the surface of the wire before using, by means of a leadous electrolytic process. The molybdenum wire so manufactured is nonuniform in diameter and nonuniform in mechanical properties. **I**n some places it lacks adequate plasticity, making its winding on automatic machines difficult and leading to high rates of spoilage in winding grids. A serious shortcoming is the ease of oxidation of molybdenum wire during assembly and prolonged storage. Finally, molybdenum is in short supply and is very expensive. Consequently, in connection with the development of vacuum tube technology it is necessary to find other materials that are more abundant and less expensive.

A substitute for molybdenum wire for grids may be wire of a nickel-molybdenum alloy of the type of ~~Mast~~alloy A. Alloys of this type were taken by us as the

basis for study and development of the technology of manufacturing extremely

with physical and <sup>the</sup> fine wire ~~XXXXXXXXXXXXXXXXXXXX~~ mechanical properties <sup>required of a substitute for</sup> ~~allowing it to replace~~

molybdenum wire for the grids of electron tubes.

To determine more precisely the chemical composition we melted nickel-molybdenum alloys with varying <sup>content of molybdenum</sup> ~~XXXXXXXXXXXXXXXXXXXX~~ (in the range from 10 to 30%) and of nickel (from 66 to 69%). The silicon content was considerably lower than in the alloys hastelloy A and B. The manganese content was varied from 0.35 to 2.00% in order to study the influence of this metal on hot deformation. Table 1 gives the chemical composition of several experimental heats.

Table 1

Chemical Composition of Nickel-Molybdenum Alloys of  
Experimental Heats, %

Heat  
No.

C

Fe

remainder

In melting the experimental nickel-molybdenum alloys, measures were taken to obtain a pure metal with the lowest possible gas content, which is of great importance for alloys with a high resistance to deformation.

The experimental alloys were melted <sup>in magnesite crucible</sup> in a 40-kg high-frequency furnace <sup>at</sup> ~~in magnesite crucibles~~ of the experimental plant of the Central Research Institute for Ferrous Metallurgy. High grade pure materials were selected for the charges: electrolytic nickel of grade "extra" or "000", metallic molybdenum, metallic manganese of grade Mrl, crystalline silicon, metallic chromium, and technically pure armco iron.

A basic slag consisting of 65% CaO; 25% MgO and 10% fluorspar was used <sup>in the smeltings.</sup> After melting of the charge, diffusional deoxidation with borlime (a mixture of lime with aluminum powder) <sup>through</sup> the slag was employed. The subsequent direct deoxidation (after the diffusional deoxidation) was accomplished by metallic ~~manganese~~ <sup>manganese</sup> and crystalline silicon. Finally, ~~XXXXX~~ <sup>before</sup> teeming. ~~XXXXX~~ the metal was deoxidized by a nickel-magnesium master alloy (15% Mg) and with silicocalcium.

After melting the charge, a vacuum of 15 mm Hg was established in the furnace. The metal was poured at 1370 - 1400°C into heated ingot molds through hot freshly ignited ~~runners~~ <sup>runners</sup>.

The technology of melting, ~~XXXXX~~ <sup>using a clean</sup> charge, boiling in a rarefied atmosphere, thorough deoxidation and proper pouring, should assure the production of a sound and dense ~~ingot~~ <sup>ingot, free of porosity.</sup>

### Hot Deformation

Nickel-molybdenum alloys have an exceedingly high resistance to deformation in the hot state. At molybdenum contents over 20% these alloys may be deformed in a narrow range of temperatures.

The ingots were heated in a gas furnace to 1220 - 1250°C, and the ~~XXXX~~ temperature at the end of rolling the ingots was 1020 - 1060°C. Experimental forging of these alloys showed that the ~~following~~ <sup>following</sup> measures of precaution had to be taken for successful hot deformation: ~~heating~~ <sup>heating</sup> the ingots and ~~the~~ rough forgings in a sulfure-free medium; the holding time at high temperatures (1230 - 1250°C) must not be prolonged; the flame in the gas furnace must be slightly reducing; and contact of the flame with the metal must be avoided. Failure to observe these precautionary measures led to surface cracks during forging.

401

The forging of the ingots proceeded satisfactorily except for heats with over 28% Mo (heats No. 409 and 410). The ingots from these heats fractured during forging in spite of the elevated manganese content. The narrow range of temperatures at which the metal is ~~fractured~~ <sup>fracture</sup> makes it necessary to preheat the ingots, to use rough forgings of small ~~weight~~ <sup>weight</sup> and to force the ~~metal~~ <sup>metal</sup> as rolling ~~metal~~ <sup>metal</sup>.

The forged and cleaned rough forgings (squares of 24 - 36 mm) were rolled ~~into a wire rod~~ <sup>into a wire rod</sup> (8 mm circle) on the 300 mm rolling mill of the "Elektrostal'" Plant. The rolling was done with ~~the~~ <sup>the</sup> mixed grooving (circle-oval, square-oval) adopted at the plant for rolling alloy grades of steels on the 300mm duplex-duo



The curves of Fig.1 show the variation of the tensile strength and elongation of wire of a nickel-molybdenum alloy containing 25% Mo (NIMO25) with the heating temperature. It will be seen that with increasing temperature above 1150°C the elongation falls rapidly, in connection with the overheating of the metal. The holding time at high temperatures should be minimum.

Prolonged holding <sup>at temperature</sup> often led to rupture of the wire coil. For <sup>coiling</sup> the ~~wire rod~~ <sup>wire rod</sup> (circle 5 - 8 mm, weight 5 - 10 kg), holding at 1150°C for 10 min was entirely sufficient for a successful anneal. ~~XXXXXX~~ <sup>The intermediate</sup> anneals were run at lower temperatures.

Wire of diameter less than 1.0 mm, to eliminate the <sup>pickling</sup> ~~pickling~~ process, and also to decrease the gas content, ~~XXXXXX~~ <sup>was</sup> annealed in a hydrogen furnace at 1050 - 1030°C.

To remove the scale from the ~~surface~~ <sup>after</sup> ~~XXXXXX~~ heat treatment, wire of diameter over 1.0 mm was <sup>pickled</sup> ~~pickled~~ in a solution of 12 - 15% sulfuric acid and 3.5% nitric acid, which is ordinarily used for alloys with a high nickel content. The ~~pickling~~ <sup>pickling</sup> temperature was 60 - 80°C. The ~~pickled~~ <sup>pickled</sup> metal was thoroughly rinsed, first with hot water and then with cold. Before drawing, the wire, after ~~pickling~~ <sup>pickling</sup>, was stored in a dry and warm place not less than 24 hr. The intermediate <sup>held to</sup> ~~anneals~~ <sup>anneals</sup> of the wire ~~must~~ be run in a protective atmosphere to avoid loss of metal in ~~pickling~~ <sup>pickling</sup>.

~~For~~ <sup>relatively</sup> nickel-molybdenum alloys with up to 28% Mo, ~~are~~ <sup>are</sup> ~~XXXXXX~~ <sup>XXXXXX</sup> a cold deformation is relatively easy, not harder than <sup>for</sup> ~~high~~ <sup>high</sup>-alloy grades of steel (~~stainless steels and nichrome~~). The lower the molybdenum content of the



Fig.2 - ~~Variation of~~ Mechanical Properties of Cold-Drawn

Wire of Alloy with 25% Mo (a) and 20% Mo (b) <sup>versus</sup> ~~with the~~ Reduction

a: 1 - Tensile strength; 2 - Yield strength; 3 - Elongation

b: 1 - Tensile strength; 2 - Elongation

●—● Heat No.411; ●—● Heat No.412

a) Tensile strength  $\sigma_s$ , kg/mm<sup>2</sup>; b) Reduction, %; c) Elongation, %

403

alloy, the easier the cold deformation proceeded. It was not necessary to use

any coating of the wire surface in drawing. A mixture of soap powder with

sulfur (flowers of sulfur) was used as a lubricant for drawing on the ~~surface~~ <sup>full blocks</sup>

and intermediate ~~drawing-downs~~ <sup>blocks</sup>. In drawing the fine wire, only soap powder was

used on the fine drawing ~~downs~~ <sup>blocks</sup>.

The partial reductions ranged from 12 to 20%. The total reductions ~~from~~

ran from 55 to 85%.

Nickel-molybdenum alloys work-harden rapidly during ~~cold~~ deformation. Here the sharp fall of elongation characteristic ~~of~~ all austenitic steels takes place. Figure 2 shows the variation in the mechanical properties of cold drawn wire of alloys with 25 and 20% Mo as a function of the reduction. It also shows the variation in plasticity, as characterized by the elongation. In spite of the rapid work hardening, wire of nickel-molybdenum alloys free of additional elements has a large margin of plasticity, so that great total reduction in wire drawing can be allowed.

#### Manufacture of Extremely Fine Wire

~~are~~ Nickel-molybdenum alloys ~~are~~ drawn to <sup>the</sup> finest micron sizes at plants of the radio industry. Such wire must be annealed only in <sup>conventional</sup> furnaces with a protective atmosphere. Wire is heated in <sup>style</sup> through hydrogen furnaces at plants of the radio industry by the passage of an electric current through the wire <sup>through</sup> by ~~means of~~ mercury contacts. To assure uniform heating of the wire, the ~~close~~ furnace is then brought to the required temperature by means of electrical resistance elements.

The drawing from 0.2 mm to 0.070, 0.030 mm was accomplished on multiple ~~frames~~ <sup>frames</sup> through diamond dies. The total reductions in many cases were brought up to 80%. An emulsion of amine soap prepared from chemically pure oleic acid and triethanolamine was used as the lubricant. This lubricant has a low ash content, which is very important for <sup>the</sup> cold-drawn wire used in vacuum tubes.

### Manufacture of Grids

Several types of grids for various types of vacuum tubes were manufactured from the ~~above~~ extremely fine wire <sup>sodium</sup>. The grids were made on automatic machines which cut out recesses on the ~~XXXXXXXXXX~~ <sup>crosspieces</sup> wound the wire in them and ~~beaded~~ <sup>beaded</sup> ~~to attach~~ <sup>onto</sup> the coils ~~to~~ the crosspieces. To have the wire successfully wound automatically, it must be given the proper anneal in the appropriate plastic condition.

For nickel-molybdenum alloy with 25% Mo, for instance, annealing conditions have been established in which, at diameter 0.70 mm, a breaking strength of 310 - 340 gm and 25 - 30% elongation is obtained.

<sup>The grids</sup>  
Grids made of wire of nickel-molybdenum alloys with 20 - 28% Mo, after annealing in hydrogen, <sup>held</sup> ~~maintain~~ their shape and had all the necessary properties.

### Microstructure

According to the equilibrium diagram of the ternary iron-nickel-molybdenum alloy, alloys with 50 to 80% Ni and 20 to 30% Mo at 20°C consist of a solid  $\delta$ -solution and intermetallic compounds.

The microstructure of nickel-molybdenum alloys in the cast condition consists of austenite polyhedra with <sup>precipitates</sup> ~~aggregations~~ of the excess phase (Fig.3,a).

The microstructure of an annealed wire <sup>rod</sup> consists of coarse grains of solid  $\delta$ -solution with <sup>precipitates</sup> ~~aggregations~~ of the excess phase <sup>inside</sup> ~~within~~ the grains (Fig.3,b).

Mechanical and Physical Properties of Wire of Nickel-Molybdenum Alloys(a) Tensile Strength at High Temperatures

Since wire for radio-tube grids must maintain high strength and rigidity at elevated temperatures, we determined the variation of the tensile and modulus of elasticity with increasing temperature.

The elevated-temperature tensile test was run on specimens 0.8 mm in diameter on a GZIP half-ton tensile machine. The wire ~~is~~<sup>was</sup> heated by passing a 24 volt DC through it. This current was obtained through a 14 kv selenium rectifier of type VSA-6. The current strength was regulated by a rheostat. One lead was connected directly to a sponge insulated from the machine, and supporting the specimen, and the other lead to the machine. The temperature at break to which the specimen was heated ~~XXXXXX~~ was measured by a thermocouple attached to its surface. Table 2 shows the tensile strength of the wire ~~as from~~ several heats with varying molybdenum content, heated to temperatures from 200 to 750°C. At over 20% Mo the wire maintains its strength at temperatures up to 700 - 750°C. At less than 20% Mo, the fall in strength at temperatures over 500°C is sharper.

2755

a

b

Fig.3 - Microstructure of Nickel-Molybdenum Alloys (NIMO). 400 x  
a - Cast specimen of NIMO25; b - Specimen of hot-rolled and  
annealed NIMO25 alloy .

Table 2

## Tensile Strength of Nickel-Molybdenum Alloys at Various Temperatures

Heat No.	Mo Content, %	Tensile Strength, kg/mm <sup>2</sup> , at following Temperatures, °C	
		20	200
757			

406

(b) Modulus of Elasticity at High Temperatures

The modulus of elasticity of nickel-molybdenum alloys at room and elevated temperatures, characterizing the rigidity of the specimens, was determined by the resonance method on a special instrument at the Central Research Institute for Machine Building. The test consists in the excitation of transverse vibrations in the vertical plane of a circular specimen, and in the measurement of the frequency of such vibrations.

Table 3 gives the test results on specimens of various nickel-molybdenum alloys annealed before the test. The modulus of elasticity of nickel-molybdenum alloys, is the same as that of high-carbon grades of steel, and is higher than that of many well-known alloys and high-alloy grades of steel [XXXXX]

(17.000 - 20.000 kg/mm<sup>2</sup>)\*.

Table 3

Modulus of Normal Elasticity of Experimental Nickel-Molybdenum  
Alloys at Various Temperatures

Heat No.	Modulus of Normal Elasticity, kg/mm <sup>2</sup> , at the following Temperatures, °C		
	20	160	200
757			
346			

With increasing temperature, the modulus of elasticity of nickel-molybdenum alloys decreases. At over 20% Mo, this decrease is slight by comparison with other alloys and grades of steel. At 600°C, the modulus of elasticity decreases 13%, while, according to Roberts, the decrease for most alloys amounts to 18 to 24%; at 800°C it ~~is~~ respectively 19 - 20% as against 25 - 40%.

---

\* ~~Some~~ Data on the moduli of elasticity of various grades of steel and alloys at various temperatures, likewise determined by the resonance method, are given by Roberts ~~and~~ Northcliffe in the Journal of the Iron and Steel Institute for June 1947.

Physical Properties of the Alloys

To judge the suitability of the wire of the heats investigated for radio tube grids, a number of its physical parameters had to be determined. We determined the following physical constants of nickel-molybdenum alloys, with varying molybdenum contents: specific gravity, resistivity, temperature coefficient of resistance, temperature coefficient of thermal expansion at temperatures up to 800°C, and thermal conductivity at temperatures up to 100°C.

Specific Gravity

It was necessary to determine the specific gravity because the gauge of the finest wire is not measured by a micrometer but is ~~controlled~~ <sup>found</sup> instead, ~~from~~ <sup>from</sup> the weight of specimens of accurately computed length. The following ~~are~~ <sup>were</sup> the values for the specific gravity of alloys of the experimental heats:

Heat No.	Sp.gr
413	

The specific gravity ~~is~~ <sup>was</sup> the higher, the higher the molybdenum content. Depending on small variations in the composition, the specific gravity of alloy NIM025, containing 24 - 28% Mo, ranged from 9.00 to 9.18.

Resistivity

The resistivity of <sup>the</sup> nickel-molybdenum alloys was determined on a Wheatstone bridge on specimens of annealed wire 0.2 mm in diameter.

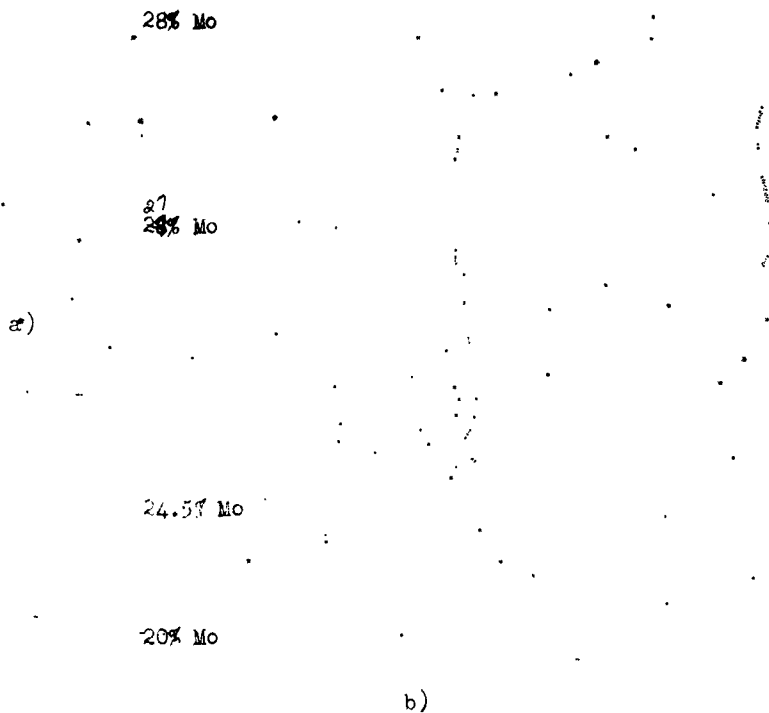


Fig.4 - Variation of Resistivity of Nickel-Molybdenum Alloys  
with ~~As a Function of~~ the Molybdenum Content and the Temperature

a) Resistivity, ohms/mm<sup>2</sup>/m; b) Temperature, °C

Alloys containing 65 - 69% Ni and over 20% Mo possess a very high resistivity, from 1.20 to 1.45 ohm/mm<sup>2</sup>/m. With increasing molybdenum content, their resistivity rises. Figure 4 shows the <sup>temperature dependence</sup> ~~variation~~ of the resistivity of

nickel-molybdenum alloys with varying molybdenum content, as a function of the

~~temperature.~~ The temperature

coefficient of resistivity falls

sharply with increasing molybdenum

content (Fig.5). At 27 - 28% Mo,

the temperature coefficient ~~of~~ ~~resistivity~~ of

resistivity of the nickel-molybdenum

alloy approaches that of ~~the~~ ~~chromium-aluminum alloy No.2~~

chromium-aluminum alloy No.2 used

for resistors, and in ~~the finest~~ ~~miniature~~

sizes can replace it in miniature

elements.

a)

b)

Fig.5 - ~~Temperature~~ Temperature  
Coefficients of Resistance of  
Nickel-Molybdenum Alloys as a  
Function of the Molybdenum Content  
(Ni = 67 - 68%)

a) Temperature coefficient of

resistivity,  $\alpha \times 10^{-6}$ ;

b) Molybdenum content, %

Coefficient of Linear Expansion

The thermal coefficient of linear

expansion of nickel-molybdenum alloys

was determined on a Leitz

differential dilatometer in the

temperature range from 20 to 800°C

on standard anneal ~~specimens~~ <sup>specimens</sup> 3.6 mm in diameter. ~~Its value is~~ <sup>It was</sup> not high by

comparison with steel and other alloys, especially for alloys with high

molybdenum content, but ~~it is~~ <sup>it is</sup> still almost double ~~the~~ <sup>the</sup> value for molybdenum.

a)

b)

of  
 Fig.6 - Temperature Dependence of Coefficients of Linear  
 Expansion of Nickel-Molybdenum Wire

a) Coefficient of linear expansion,  $\alpha \times 10^{-6}$ ;

b) Temperature, °C

409

Figure 6 shows the curves of variation of the temperature coefficient of expansion of the nickel-molybdenum alloys with rising temperature.

#### Thermal Conductivity

The coefficient of thermal conductivity of the alloys up to 100°C was determined on a Tomashov-Fridman instrument on specimens 6 mm in diameter and 150 mm long. The following were the values of the thermal conductivity, cal/cm-sec-°C:

Heat No.

757

The thermal conductivity of the nickel-molybdenum alloy is very low by the comparison with that of pure metals, ~~and~~ especially that of molybdenum, which has a coefficient of thermal conductivity of 0.35 cal/cm sec °C.

Thermal conductivity is one of the most important characteristics of an alloy for radio-tube grids. The rapid removal of heat from a grid is one of the necessary conditions ~~for~~ normal operation. The low thermal conductivity of nickel-molybdenum alloys, like that of all other alloys, prevents ~~their~~ substitution ~~for~~ molybdenum or tungsten ~~in the grids of radio-tubes~~ <sup>in certain</sup> grids.

Where the grid becomes heated and it is impossible to remove the heat by means of cross ~~sections~~ <sup>pieces</sup> or by increasing the radiation ~~by using~~ <sup>by using</sup> various coatings, grid thermo-currents arise, ~~and disturb the proper operation of the tube~~ <sup>interfering with normal tube operation.</sup>

#### Manufacture of Grids

Grids manufactured from experimental batches of nickel-molybdenum alloy wire were assembled in several types of electron tubes: In testing and comparing them with tubes of the same type with grids of the material ~~used at~~ <sup>then</sup> the plant, satisfactory results were given by tubes with grids of wire of nickel-molybdenum alloys containing over 20% Mo. The consumer plants prefer the use of wire of alloys containing 67 - 69% Ni and 24 - 25% Mo, since their rigidity is higher. The wire of this composition required by the radio industry, 0.2 mm in diameter, is being delivered by the experimental plant of the Central Research Institute for Ferrous Metallurgy, and in the finest gages, by the Beloretskiy and "Elektrostal'" plants.

Wire of alloy NIM025 successfully substitutes for molybdenum wire in many types of electron tubes. In fine cross sections, it possesses high strength ~~at~~ room and elevated temperatures. At the same time it <sup>also</sup> possesses good impact strength, <sup>facilitating</sup> ~~permitting~~ automatic winding of grids, ~~to be easily accomplished.~~ The grids wound with this wire have adequate rigidity to <sup>the</sup> resist deforming forces during assembly, and maintain their shape and size during operation and during the degassing of elements in the tube at high temperatures. Wire of alloy NIM025 has a number of advantages over molybdenum wire. It does <sup>not</sup> oxidize in the air, while molybdenum does show considerable oxidation during prolonged storage and during the <sup>sealing</sup> ~~winding~~ of the tubes. In contrast to molybdenum wire, it can be drawn cold at high speeds on multiple <sup>frames.</sup> ~~machines.~~ The wire produced is light, uniform in diameter and uniform in mechanical properties over the entire length of the <sup>coil.</sup> ~~spool.~~ The spoilage of grids of alloy NIM025 during winding is negligible in comparison with grids of brittle, <sup>irregular and nonuniform</sup> ~~nonuniform~~ molybdenum wire.

Radio tubes with grids of wire of alloy NIM025 are <sup>equivalent</sup> ~~equivalent~~ in service life and other parameters - distribution of anode current, transconductance characteristics and emission - to tubes of the same type with fickedized molybdenum.

Nickel-molybdenum alloys have found use in the radio industry not only for grids but also for other components. The technology of ~~manufacture of~~ cold-rolled strip 0.15 mm thick (of alloys NIM020 and NIM025) which can be used for the <sup>discharge</sup> ~~manufacture~~ of new types of vacuum tubes have been developed. The basic requirement in this case is the service life of the <sup>discharge</sup> ~~manufacture~~, which is

determined by testing <sup>20</sup> the fatigue limit ~~of the membrane~~ by ~~XXXXXXXXXXXX~~ <sup>the breaking</sup>  
 its vacuum seal by vibrations on a special instrument.

Cold rolled strip after annealing and pickling <sup>and</sup> likewise <sup>to draw into wire</sup> ~~passed into wire~~  
 without difficulty. The total reduction amounted to 80 - 85%.

#### Nickel-Tungsten Wire for Grids in Radio Tubes

In view of the fact that molybdenum is expensive and in short supply, the use of <sup>a</sup> nickel-base molybdenum-free alloy has been proposed for the grids of electron tubes. Tungsten is an element which is a successful substitute for molybdenum in many alloys and grades of steel. It is less scarce than molybdenum and is also cheaper. Several heats of nickel-tungsten alloys were run in a high frequency furnace, using the same precautions and the same technology as for the nickel-molybdenum alloys (Table 4).

No data whatever can be found in the literature on the properties of nickel-tungsten alloys, but our very first experimental studies showed their resistance to deformation in the hot condition to be as great as that of the nickel-molybdenum alloys. For successful forging, likewise, it was necessary to use a clean, dense, well deoxidized ingot. It <sup>had to</sup> ~~must~~ be heated to a high

411

Table 4

Chemical Composition of Experimental ~~Nickel~~-Base Alloys of Tungsten, %

Heat No.	C	Mn	Si	Ni	W
----------	---	----	----	----	---

temperature for forging and rolling. - 1200 - 1240°C. In the range 600 - 1000°C, nickel-tungsten alloys are as brittle as nickel-molybdenum alloys.

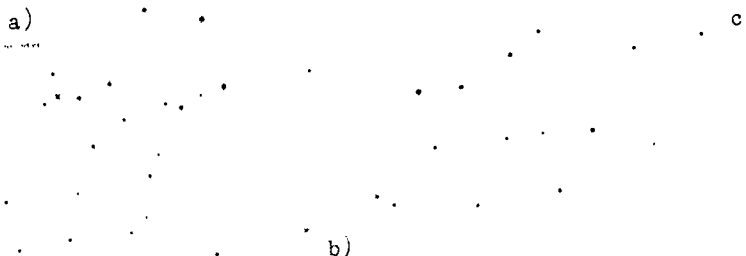


Fig.7 - Variation of the Mechanical Properties of Nickel-Tungsten Alloys ~~as a function of~~ <sup>with</sup> the Annealing Temperature (Heat No.234);

1 - Tensile strength; 2 - Elongation

a) Tensile strength, kg/mm<sup>2</sup>; b) Temperature, °C; c) Elongation, %

Figure 7 shows the variation of the tensile strength and elongation of nickel-tungsten alloy wire with 25% ~~as a function of~~ <sup>with</sup> the annealing temperature.

It will be seen that the optimum annealing conditions for this alloy are

heating to the range 1050 - 1150°C. After heating at these temperatures,

followed by rapid cooling, nickel-tungsten alloy wire has a tensile strength

under 100 kg/mm<sup>2</sup> and an elongation of 30 - 36%. But ~~already on heating to~~ <sup>only</sup>

900 - 950°C <sup>still gives</sup> a plastic wire for cold deformation with elongation 25 - 30% ~~can~~

~~be obtained.~~

At tungsten content from 10 to 15%, the optimum annealing conditions are heating to the range 1000 - 1100°C.

-412

*Descaling of*  
 The ~~removal of the scale from~~ <sup>the</sup> surface of low-tungsten wire was accomplished by ~~pickling~~ <sup>pickling</sup> in a solution consisting of 10% sulfuric acid, 5 - 6% of hydrochloric acid and 2 - 25% of nitric acid, at 65 - 75°C, followed by immersion for several minutes in a hot 10% solution of calcined soda.

In spite of the fact that annealed nickel-tungsten wire has lower elongations than wire of nickel-molybdenum alloys, it is considerably more plastic and can be drawn to the finest gages without trouble.

The character of the curves in Fig.8 shows that nickel-tungsten alloy wire (NIV025) does not work harden during deformation *as much as* ~~to the same extent as~~ <sup>as much as</sup> nickel-molybdenum alloy wire (NIMO25) *does*.

Fig.8 - ~~Variation of~~ Mechanical Properties of Nickel-Molybdenum Alloy as a Function of the

Reduction:

- 1 - Tensile strength, <sup>heat</sup> ~~NIV~~ No.233;  
 2 - Tensile strength and elongation, ~~heat No.233~~ <sup>heat No.236</sup>  
 3 - Tensile strength, heat No.236  
 a) Tensile strength, kg/mm<sup>2</sup>;  
 b) Reduction, %; c) Elongation, %

Mechanical and Physical Properties with Nickel-Tungsten Alloys

*Winkler-Vogel phase diagram of the*

According to the ~~equilibrium diagram~~ of ternary iron-nickel-tungsten

~~system~~  
~~alloys prepared by Winkler and Vogel~~, alloys ~~at room temperature~~ with 60%

of nickel and 10 to 26% of molybdenum <sup>*at room temperature*</sup> consist of a  $\delta$ -solid solution and

intermetallic compounds, iron-tungsten and nickel-tungsten. Figure 9 shows

the microstructure of annealed nickel-tungsten alloy wire with 25% W, consisting

of coarse grains of solid  $\delta$ -solution with segregation of the excess phase

inside the grains.

Mechanical Properties of Nickel-Tungsten Alloys

The tensile strength of nickel-tungsten alloy wire at elevated temperatures

~~the~~ *the* GZIP

was determined on ~~the~~ tensile machine by the method described above.

Table 5 gives the results of the tests.

413

Table 5

Tensile Strength of Nickel-Tungsten Alloys

Heat No.	Tensile Strength, kg/mm <sup>2</sup> , at Various Temperatures, °C									
	20	200	270	360	420	450	600	700	750	800

At over 20% W,  
 the tensile strength, with over 20% W on increasing the temperature to 600°C,  
 decreases slightly (about 20%) from the initial strength, but even at 800°C  
 it still remains rather high. The strength of <sup>the wire from</sup> ~~the~~ heat No. 236 with 25.8% W  
~~was~~ almost as high as that of alloy NIM025 at these temperatures, and ~~is~~ higher  
 than that of a nickel-molybdenum alloy with 20% Mo.

Fig. 9 - Microstructure of Annealed Specimen of Nickel-Tungsten Alloy  
 (25% W). 400 x

Table 6 gives the results of ~~the~~ <sup>a</sup> determination of the modulus of normal  
 elasticity at room temperature and elevated temperature ~~the~~ <sup>for</sup> already annealed  
 specimens.

Table 6

## Modulus of Normal Elasticity of Nickel-Tungsten Alloys

Heat No. 20 Modulus of Elasticity,  $\text{kg/mm}^2$ , at Various Temperatures,  $^{\circ}\text{C}$

The modulus of elasticity of nickel-tungsten alloys at room and elevated temperatures is as high as for nickel-molybdenum alloys. It is particularly high for the alloy with 25% W,  $18000 \text{ kg/mm}^2$  at  $800^{\circ}\text{C}$ , just as high as most alloys at room temperature.

Physical Properties of Nickel-Tungsten Alloys

We determined the physical properties by the same methods as for nickel-molybdenum alloys.

Specific gravity, resistivity and thermal conductivity of the following

alloys:

Heat No.	233	234	235	236
Tungsten content				
Specific gravity				
Resistivity, $\text{ohms-mm}^2/\text{m}$				
Thermal conductivity, $\text{cal/cm-sec-}^{\circ}\text{C}$				

With increasing tungsten content, the specific gravity of the alloy increased. Its mean value was 10.235 for five heats of the alloy with 25% W (NIVO25). The resistivities of nickel-tungsten alloys increase<sup>with</sup> ~~increasing~~ <sup>the</sup> tungsten content.

Figure 10 shows the ~~XXXXXXXXXX~~ <sup>temperature</sup> dependence of the resistivity of the alloys. The temperature coefficient of these alloys is higher than that of nickel-molybdenum alloys, but, beginning at 400°C, their resistivity remains almost unchanged.

The thermal conductivity of nickel-tungsten alloys up to 100°C was determined on a Tomashov-Fridman instrument.

415

One specimen of an alloy containing 25% W (NIVO25) was tested for thermal conductivity at temperatures up to 800°C at the Central Research Institute for Machine Building on an instrument designed on the Kohlrausch principle. In this instrument the test specimen was heated by an electric current in vacuo; the

a)

a)

b)

b)

Fig.10 - Temperature Dependence of  
the Resistivity of Nickel-Tungsten  
Alloys

1 - Heat No.233; 2 - Heat No.234;

3 - Heat No. 235; 4 - Heat No.236

a) Resistivity, ohm/mm<sup>2</sup>/m;

b) Temperature, °C;

Fig.11 - Temperature Dependence  
of Thermal Conductivity of Alloy  
NIVO25

a) Thermal conductivity  $\lambda$ ,  
cal cm sec °C;

b) Temperature, °C

quantity of heat conducted was determined from the potential difference. The  
electrical  
~~electrical~~ conductivity of the alloy was determined at the same time.

Table 7 and Fig.11 show the results of the tests.

Table 7

Results of Determination of Electrical Conductivity and  
Thermal Conductivity of Alloy NIV025 at Various Temperatures

	Test Temperature, °C				
	126.7	205	342	448	600
Electrical conductivity	0.811				
Thermal conductivity cal/cm-sec-°C					

With increasing temperature, the thermal conductivity of the alloys considerably increases. The rise in thermal conductivity in this case is linear, as will be seen from Fig. 11. The linear and considerable rise in

the thermal conductivity of nickel-tungsten alloy during heating is its

416 advantage over other alloys, whose thermal conductivity <sup>generally</sup> increases, but sometimes even decreases, with increasing temperature. This property of NIVO alloy

should expand the possibility of its use for grids of various types of electron tubes.

Table 8 gives the thermal <sup>coefficients</sup> ~~coefficients~~ of linear expansion <sup>of the nickel-tungsten</sup> ~~coefficients~~

*alloys.*  
~~alloys.~~

Table 8

Coefficient of Linear Expansion ( $\alpha \times 10^{-6}$ ) of Nickel-Tungsten Alloys

Heat No.	Temperature, °C							
	20-100	20-200	20-300	20-400	20-500	20-600	20-700	20-800
233								
234								
236								

Resistance of Nickel-Tungsten Alloys to Corrosion

The corrosion resistance of nickel-molybdenum alloys under atmospheric conditions evoked no doubts whatever, since similar alloys are used in the chemical industry as corrosion-resistant. Nickel-tungsten alloys containing 60% Ni and 10 - 21% W have not heretofore been used in industry, and there are no data on their resistance to corrosion. In dry air, like all other high-nickel alloys, they do not oxidize. To determine the corrosion resistance of the nickel-tungsten alloys under investigation, under atmospheric conditions, specimens of wire of these alloys were tested for seven days under the following conditions: from 9 to 13 hr, rocking in a variable load apparatus; from 13 to 17 hr, in the air, from 17 to 4 hr, in tap water.

For purposes of comparison, specimens of wire of nickel-molybdenum alloys with 20 and 27% Mo were tested ~~under these same~~ <sup>under these same</sup> conditions. Table 9 gives the losses in weight after the tests. According to the results obtained, the corrosion resistance of nickel-tungsten alloys ~~under humid atmospheric~~ <sup>under humid atmospheric</sup> conditions is not poorer than that of nickel-molybdenum alloys under the same conditions.

Under prolonged storage and during the assembly of electron tubes with grids of wire of nickel-tungsten alloys, no oxidation was noted.

Table 9

Results of Tests of Alloys NIVO and NIMO for Resistance  
to Corrosion

Specimens of Alloys	Wire Diameter, mm	Weight before Testing, gm	Weight after Testing, gm	Weight Losses		
				gm	%	cm <sup>2</sup> /hr
NIVO of heat:						
No. 236						
No. 235						
No. 234						
NIMO20						
NIMO25						

Table 10 gives, for comparison, the mechanical and physical properties  
of annealed wire for radio-tube grids, made of molybdenum alloys NIMO and NIVO.

Table 10

Comparative Mechanical and Physical Properties of Annealed  
Wire of Molybdenum and of Alloys NIMO and NIVO

Material	$\sigma_b$ , kg/mm <sup>2</sup>	$\sigma_s$ , kg/mm <sup>2</sup>	$\sigma$ , %	$\delta_b$ , kg/mm <sup>2</sup>		E, kg/mm <sup>2</sup>	
				at 500°C	at 800°C	at 200°C	at 800°C
Molybdenum wire							
NIMO25							
NIMO20							
NIVO25							
NIVO20							

Material	Thermal Conductivity cal/cm-sec°C	Temperature Coefficient of Thermal Expansion, $\alpha \times 10^{-6}$	Resistivity, ohm/mm <sup>2</sup> , 20°C	Melting Point, °C
Molybdenum wire				
NIMO25				
NIMO20				
NIVO25				
NIVO20				

418

Test of Nickel-Tungsten Alloy Wire in Radio Tubes

The first tests of grids made of nickel-tungsten alloys with 21 and 25% W in 200 type 2K2Zh tubes yielded satisfactory results for all parameters. Favorable results were also obtained after testing for service life. All tubes tested showed a drop in anode current, transconductance and rise in emission within the established standards after 500 hr of service. The tests were repeated on 10000 tubes with grids made from an industrial batch of nickel-tungsten alloy wire with 24 - 26% W (NIVO25). The quality of the tested tubes was found to be equivalent to that of the current production. The mean value of their parameters was the same. The percent of output of satisfactory tubes in a sample was the same as that in the current production, 90.5%. Favorable results were also given by a test of NIVO25 wire for grids of other types of tubes at other plants of the radio industry.

As a result of the tests run and of the fact that NIVO wire deforms  
 very easily in the cold condition, NIMO alloy wire should ~~XXXXXXXXXXXX~~ be replaced by NIVO  
~~XXXXXXXXXXXX~~ wire.

NIVO wire has also found use for other components in several types of radio tubes.

#### Conclusions

1. The chemical composition of nickel-molybdenum alloys (NIMO) has been  
 more precisely determined, their properties have been studied, and a technology  
 developed for the manufacture of extremely fine wire from this alloy for  
 radio tube grids to replace wire of ~~XXXXXXXXXXXX~~ molybdenum, which  
 is in short supply and  
 is difficult to work. The technology of producing NIMO wire has been  
 introduced into industry.

2. Compositions <sup>for</sup> nickel-base molybdenum-free alloys with tungsten  
 have been selected, their properties have been studied, and the technology of  
 production of extremely fine wire from these alloys has been developed. Grids  
 made of NIVO alloy wire are as good as grids of NIMO or molybdenum. The  
 technology of production of NIVO alloy wire has been <sup>industrially developed.</sup>  
~~introduced into industry.~~

## STRUCTURAL TRANSFORMATIONS IN NICKEL-BASE ALLOYS

by

Engineer L.N.Zimina and Professor M.V.Pridantsev,  
 Doctor of Technical Sciences

The extensive industrial use of nickel-base heat-resisting alloys and the design of new super-alloys demands a profound understanding of the structural transformations taking place during heat treatment and operational use of the alloys.

Most heat-resisting alloys <sup>undergo</sup> dispersion hardening by segregation of intermetallic phases. Great interest therefore attaches to the systematic study of <sup>the</sup> phase diagrams of complex and simple systems.

The first phase diagram of the system Ni-Ti was drawn by Vogel and Wallbaum (Bibl.1), and was based on X-ray diffraction and microstructural studies. According to these authors the <sup>solubility</sup> ~~solubility~~ of titanium <sup>in</sup> and nickel was 2.8 - 3.0 Wt.% at 800°C. The titanium they used, however, was not sufficiently pure (95%), and this fact casts doubt upon the position of the solubility limit of titanium <sup>in</sup> and nickel.

In 1952 Taylor and Floyd (Bibl.2) published a detailed study of the system Ni-Cr-Ti, ~~giving~~ giving the solubility of titanium <sup>in</sup> ~~and~~ nickel at 750 and 1150°C as 9.4 at.% ~~as~~ (7.8 wt.%) and 13.0 at.% ~~as~~ (10.8 wt.%), respectively.

At a titanium concentration beyond these limits, the intermetallic phase Ni<sub>3</sub>Ti (?), with a hexagonal close-packed lattice, is segregated. This phase is observed on polished sections in the form of very fine lamellae. Subsequent studies by Yu.A. Bagaryatskiy and Yu.D. Tyapkin (Bibl.3) established the solubility limits of titanium in nickel at 800 and 1100°C and confirmed the data given by Taylor and Floyd.

The present study was undertaken with the object of determining the solubility limit of titanium <sup>in</sup> ~~and~~ nickel at lower temperatures, of studying the structural transformations during aging of Ni-Ti and Ni-Ti-Al alloys of composition close to the solubility limit at 600 - 800°C, and of studying the structure of several industrial alloys of the system Ni-Cr-Ti-Al after prolonged aging.

Starting materials of high purity were used in melting the Ni-Ti and Ni-Ti-Al alloys. They were electrolytic nickel of mark N-0 and <sup>magnesium-reduced</sup> metallic titanium, ~~prepared by the magnesium thermal method.~~ <sup>reduction</sup> The <sup>heats</sup> ~~melts~~ were run in a 10-kg induction furnace <sup>with an</sup> ~~using~~ argon ~~as the~~ protective atmosphere. Table 1 gives the chemical composition of the Ni-Ti system alloys studied.

Table 1

## Chemical Composition of Ni-Ti Alloys

Heat No.	Content of Elements, Wt.%								
	Ti	Al	Fe	Si	Mn	S	P	C	Ni
						not found		0.01	remainder
		traces							"
		"							"
		"							"
		"							"

The solubility limit <sup>of</sup> titanium ~~and~~ <sup>in</sup> nickel was determined mainly by the X-ray diffraction and microstructural methods. The X-ray diffraction patterns\* were taken by the ~~back-reflection~~ <sup>back-reflection</sup> method <sup>with</sup> copper radiation. The focusing was on the line (024) at a Bragg angle of 75 - 76°. The error of measurement of the lattice parameter was not over  $\pm 0.0006$  kX. Six diffraction patterns were ~~taken~~ taken of each specimen and the mean value of the lattice parameter was determined. The lattice parameter of the same specimen was measured first after quenching in a 10% NaCl solution ~~from~~ <sup>at</sup> 1150°C, and then after tempering for 1500 hrs at 700°C. ~~This permitted us to consider~~ <sup>consideration may therefore be</sup> the results <sup>considered</sup> rather reliable. As will be seen from the curve (Fig.1) based on the data of

\* The X-ray diffraction analysis was run under the supervision of R.M.Rozenblyum.

Table 2, the <sup>boundary</sup> ~~limit of formation~~ of the hexagonal phase  $Ni_3Ti$  at  $700^\circ C$  is 6.8 ~~wt. %~~ <sup>wt.</sup> (8.2 At. %). Figure 2 gives part of the phase diagrams of the system Ni-Ti on which the limit of separation of the hexagonal phase  $Ni_3Ti$  has been plotted from the data of other studies (Bibl. 2, 3 and 4), taking account of our own results. All points fit well on a straight line. The only exception is the point for temperature  $1150^\circ C$  obtained by Taylor and Floyd on powder specimens of an Ni-Ti alloy during a two-hour anneal, which at the high temperature could have resulted in a certain evaporation loss of titanium, but ~~the~~ <sup>equilibrium</sup> which holding time was probably not long enough to reach an ~~equilibrium~~ structure.

474

a)

 $700^\circ C - 1560$  hrs

a

b

b)

Fig. 1 - Variation of Lattice Parameter of Solid Solution after Quenching (a) and Aging (b)

a) Lattice parameter, kX; b) Titanium concentration, wt. %

Table 2

Variation of Lattice Parameter of Solid Solution and of  
Microstructure of Ni-Ti Alloys during Aging

Heat No.	Ti, wt.%	Lattice Parameter, kX, after			Structure after Aging at 700°C for 1500 hrs
		Quenching	Aging (700°C for 500 hrs)	700°C for 1500 hrs	
959	5.4	3.542	3.542		

lines strongly blurred

To bring out the microstructure of the alloys we used a reagent\* of the following composition: 3% FeSO<sub>4</sub> + 3.5% NaCl + 5% H<sub>2</sub>SO<sub>4</sub> + 88.5% distilled water, which had been developed for the electrochemical separation of the phases in Ni-Cr-Ti-base alloys. After electropolishing in concentrated nitric acid, the polished sections were electrolytically etched at a current density of 0.8 - 1.5 <sup>amp/cm<sup>2</sup></sup> ~~amp/cm<sup>2</sup>~~ During this etching, owing to the ~~different~~ <sup>different</sup> rate of electrolytic dissolution of the various structural components, parts of the solid solution with a relatively low titanium content are dissolved. The titanium-rich portions of the alloy are more stable electrochemically, and, projecting above the surface of the polished section, they become clearly visible under the microscope at magnifications

475

\* This reagent was developed in laboratory No. 41, Central Research Institute for Ferrous Metallurgy, by M.M.Shapiro and R.Ye.Grabarovskaya.

of ~~to~~ 600 - 1000 x.

In the quenched condition, all

the alloys investigated had the structure of a single-phase solid solution (Fig.3,a).

In alloys with 5.4 and 6.55% Ti at over 650°C in the phase diagram in the single-phase region, regions appear during aging which are considerably enriched in titanium

and have a distinct surface of separation from the matrix solid solution. After 25 hrs <sup>of</sup> aging at

800°C, the presence of a sharp inhomogeneity of the alloy can be

a)  
b)  
Fig.2 - Phase Diagram of Ni-Ti  
(Nickel Corner)  
a) Temperature, °C; b) Ti content,  
(atomic %)

observed under the optical microscope at high magnification (Fig.3,b). The

lower the concentration of titanium in the alloy, the smaller the ~~size~~ <sup>size</sup> and ~~quantity~~ <sup>quantity</sup> ~~of~~ ~~the~~ ~~segregated~~ ~~phase~~. This is clearly visible on the micrographs of

Fig.3 - Ni-Ti Alloy (6.55% Ti) in the Quenched Condition (a)  
and after Aging 25 hr at 800°C (b) : 2250 x

476

the alloy with 5.4% Ti (Fig.4,a) and 6.55% Ti (Fig.4,b), after aging 1500 hr at 700°C.

Fig.4 - Ni-Ti Alloy (5.4% Ti) (a) and 6.55% Ti (b)  
~~XXXXXXXX~~  
after 1500 hr Aging at 700°C. 600 x

R.B. Golubtsova and L.A. Mashkovich (Bibl.5) separated a ~~segregation in an~~ <sup>precipitate from an</sup> Ni-Ti alloy with 7.9 wt.% Ti after 100 hr tempering at 800°C <sup>(it was located</sup> on the phase diagram ~~this is found~~ in the single-phase  $\delta$ -region). They found that the anodic precipitates had a composition close to that of the chemical compound  $Ni_3Ti$ ; their titanium content was 23 - 25 at.%, but the lattice had a face-centered cubic structure with the parameter 3.581 kX. The hardening phase in the alloy EI437 has this lattice parameter.

The phase of segregation with a face-centered cubic lattice and a composition close to the compound  $Ni_3Ti$  will hereafter be termed the  $\alpha'$ -phase, to distinguish it from the  $\beta'$ -phase with the same lattice type but based on the compound  $Ni_3Al$ . It should be noted that in  $\alpha\alpha\alpha$  alloys with a low titanium content it is difficult to detect the  $\alpha'$ -phase with instruments of the present <sup>level</sup> sensitivity by such methods as the dilatometric, or by measurements of hardness and electrical resistance. In each case only a slight increment of hardness is noted during the aging of alloys with 6.5% and 7.0% Ti (Fig.5).

Alloys with higher Ti content ~~(7.0% or more)~~ <sup>precipitates</sup> show not only the ~~segregations of the  $\alpha'$ -phase but also~~ fine lamellar <sup>precipitates</sup> segregations of the  $Ni_3Ti$  ( $\eta$ ) phase with a hexagonal lattice ( $a = 5.10$  kX;  $c = 8.31$  kX;  $c/a = 1.63$ ). The presence of a considerable amount of the  $\eta$ -phase in the alloy is characterized by the appearance of a second maximum on the hardness curve. Thus, in the alloy with 9.1% Ti, during the first period of aging at 650°C, there is a gradual increase in hardness from 12 to 33  $R_c$ , primarily on account of the

segregation of the cubic  $\alpha'$ -phase (Fig.5). When the holding time is increased from 15 to 25 hr, the sharp rise of hardness to 52 R<sub>c</sub> corresponds to the formation of the lamellar  $\eta$ -phase.

In a study of the initial stages of aging of Ni-Ti alloys, Yu.M. Bagaryatskiy and Yu.D. Tyapkin (Bibl.6) found the formation of the hexagonal Ni<sub>3</sub>Ti phase to proceed in two stages. The first stage consists in the formation, in the crystal of XXX supersaturated solid solution, of regions enriched in titanium up to the composition Ni<sub>3</sub>Ti. The second stage consists in the rearrangement of the lattice in these regions into a hexagonal lattice of the segregated phase, *maintaining* with its conjugation with the impoverished solid solution, *maintained*. Consequently, in the alloys in the two-phase region ( $\gamma + \eta$ ) of the phase diagram, the cubic  $\alpha'$ -phase is metastable and in course of time must pass over into the hexagonal  $\eta$ -phase. But in alloys located to the left of the *solid* *limit of* ~~limit~~ of solubility *of*

a)

b)

c)

Fig.5 - Curves of Dispersion Hardening of Ni-Ti Alloys at 650°C.

Ti content in alloys:

1 - 6.5%; 2 - 7.0%; 3 - 7.4%; 4 - 7.67%; 5 - 9.1%

Aging time, hr;

a) Hardness,  $R_V$ ; b) ~~XXXXXXXXXXXXXXXXXXXX~~ c) Hardness,  $R_S$

titanium and nickel, the  $\alpha'$ -phase is very stable at low temperatures. Apparently its size, and perhaps also the deficit of titanium atoms, do not permit the lattice rearrangement to proceed.

The first lamellae of  $Ni_3Ti$  in the alloy with 7.0% Ti appear in several grains after 500 hr aging at 700°C (Fig.6). In alloys with a higher titanium

a

b

Fig.6 - Ni-Ti Alloy (7.0% Ti) after 500 hr Aging at 700°C. 1500 x

a

b

Fig.7 - Ni-Ti Alloy (7.4% Ti) after 500 hr Aging at 700°C.  
(a) and 1500 hr aging (b). 600 x

content, the segregation of the  $\eta$ -phase takes place at first along the grain boundaries and twinning lines in the form of parallel lamellae (Fig.7,a). With the passage of time (for example, at 1500 hr) the process now extends to the entire grain interior (Fig.7,b). The lamellae of the  $\text{Ni}_3\text{Ti}$  phase are arranged on the type of a Widmanstaetten structure.

a b

Fig.8 - Ni-Ti Alloy (7.6% Ti) after 500 hr Aging at 700°C (a) without Preliminary Deformation; and (b) with Preliminary 20.8% Extension. 300 x

Thus, in alloys located close to the solubility limit in the two-phase region ( $\gamma + \eta$ ) on the phase diagram, the structure consists for a long time of a ~~matrix~~ predominant solid solution ~~and a~~ <sup>of the</sup> ~~segregated~~ <sup>with a</sup>  $\alpha'$ -phase, mostly ~~of the~~ square shape (Fig.6,b) and a face-centered cubic lattice, and, on the other hand, a lamellar  $\eta$ -phase with a hexagonal lattice. The size of the particles of the

$\alpha'$ -phase in the alloy ~~of the~~ <sup>with</sup> 7.0% Ti after 500-hr aging at 700°C is, on the average, 0.3 - 0.6  $\mu$ . The lamellae of the  $\eta$ -phase ~~have~~ <sup>are of</sup> the most varied sizes, some of them are as long as 0.05 - 0.1 mm ~~long~~ with a width of 0.6 - 0.7  $\mu$ .

Using bulk strain hardening, the process of formation of the hexagonal Ni<sub>3</sub>Ti phase can be substantially accelerated. Figure 8 shows <sup>photo</sup> micrographs of an alloy (7.67% Ti) after aging <sup>for</sup> 500 hr at 700°C, in one case (a) immediately after quenching, and in the other case (b) after first stretching the specimen by 20.8%.

480

An ~~the~~ increase of the titanium content of the alloy and a rise in the aging temperature make the  $\alpha'$ -phase less stable. After aging an alloy with 9.1% Ti for 25 hr at 1000°C, only <sup>occasional square precipitate particles</sup> ~~occasional segregations of square phase~~ can be seen in the structure (Fig.9).

Fig.9 - Ni-Ti Alloy (9.1% Ti) after Aging 25 hr at 1000°C. 600 x



containing 5.35% Ti and 1% Al

has a two-phase structure

(Fig.11) after aging ~~for~~

200 - 500 hr at 650 - 700°C.

There is a slight decrease

in the lattice parameter of

the solid solution in this

case (from 3.5472 kX to

3.5462 kX), accompanied by

an increase in hardness

amounting to 10  $R_p$  units.

Such an alloy has a rather

Fig.11 - Ni-Ti-Al Alloy (5.35% Ti and 1% Al)

after Aging 500 hrs at 700°C. 1500 x

high resistance to heat. At 650°C, under a stress of 15 kg/mm<sup>2</sup>, the <sup>time to</sup> rupture

~~time~~ is 250 - 270 hrs, which is comparable with the long-time strength of a

two-phase ~~Ni-Ti~~ Ni-Ti alloy with 7.4% Ti, <sup>with a time to</sup> ~~which has a rupture time of~~ 185 - 200 hrs

under the same test conditions.

The dilatometric curve taken on heating quenched specimens at a rate of 1°C/min

make it possible to determine the temperature range of the transformation in

Ni-Ti-Al alloys at 1% Al. <sup>If there are no</sup> ~~In the case of absence of~~ transformations in the

alloy (3.5% Ti), the dilatometric curve in the temperature interval 500 - 900°C

is linear in character (Fig.12,a). At 5.35% Ti (Fig.12,b), in the temperature

interval 500 - 820°C, a slight shortening of the specimen is observed in

connection with the segregation of a phase of type  $Ni_3(Ti, Al)$  from the solid

solution. An increase in the titanium content to 7.5% broadens the region of existence of the second phase on heating to 930°C, while the process of coagulation and partial solution of this phase in the solid solution begins at about 750°C (the minimum on the curve of Fig.12,c).

A large number of studies of the structural transformations in alloys of the system Ni-Cr-Ti-Al have appeared in recent years in the Soviet and foreign literature, ~~especially in~~ *with special reference to* alloys of the KhN80T type (grades EI437 and NIMONIK-80). It is well known today that the hardening of type EI437 alloys is ~~accomplished on account of the segregation~~ *due to precipitation during aging* of the finely disperse phase ( $\alpha'$ ), ~~which has a~~ *precipitated particles are* ~~during aging, a phase with~~ face-centered cubic lattice and the parameter 3.58 kX. The ~~shape of the segregation is~~ *etchant* square if the ~~reagent~~ *etchant* is properly selected (Bibl.7,8,9). Nordheim and Grant (Bibl.10) consider that the ~~strengthening~~ *hardening* phase in ~~the~~ alloys of this type is based on the chemical compound  $Ni_3Al$  with a cubic lattice in which some of the aluminum atoms have been substituted by titanium atoms.

a

b

c

Fig.12 - Dilatometric Curves of Ni-Ti-Al Alloys: (a)  
1% Al, 3.5% Ti; (b) 5.35% Ti and (c) 7.5% Ti

This view is refuted by the data of chemical phase analysis\* (Table 3) showing 16 - 18 atomic percent Ti in the  $\alpha'$ -phase and only 4.5 atomic percent Al, indicating its composition to be close to that of the compound  $Ni_3Ti$  in which the titanium atoms have been partially replaced by aluminum atoms. In course of time, at a sufficiently high aging temperature, assuring the occurrence of diffusional processes, or under ~~operating~~ <sup>service</sup> conditions, under the action of

\* The chemical phase analysis was run by R.Ye.Grabarovskaya.

considerable stresses, lamellar ~~segregates~~ <sup>precipitates</sup> appear, first of all along the grain boundaries and twinning lines. Figure 13 shows ~~photomicrographs~~ <sup>photomicrographs</sup> of EI437 alloy with ~~segregates~~ <sup>precipitates</sup> of the lamellar phase. After long-time tensile tests at 700°C and stress 36 kg/mm<sup>2</sup> for 350 hr (a); after ~~operational use~~ <sup>200 hr service</sup> of the alloy for 200-hr (b) and after aging 600 hr at 800°C (c). Some authors (Bibl.11,12) tend to

483

Table 3

Composition of Metallic ~~Segregates~~ <sup>Precipitates</sup> of Alloy EI437

Heat Treatment Conditions	Yield of <del>Segregates</del> <sup>Precipitates</sup> %	<del>Composition of Segregates</del> <sup>Precipitates</sup> at. %					Ni
		Ni	Ti	Al	Cr	Fe	Ti → Al Ratio in <del>Segregates</del> <sup>Precipitates</sup>
Quench	Tempering						
1080°C, 8 hrs - water	700°C, 16 hrs	3.6					
1080°C, 8 hrs - air	the same						
1080°C, 8 hrs - with the <del>XXXXXX</del> furnace	the same						

consider that the  $\alpha'$ -phase in alloy EI437 is ~~the~~ the equilibrium product of the decomposition of the solid solution, and that there is no formation of the hexagonal Ni<sub>3</sub>Ti phase. The ~~decomposition~~ <sup>transformation</sup> of the  $\alpha'$ -phase into the compound Ni<sub>3</sub>Ti is observed only in alloys containing less than 0.04% Al. In the alloy EI437, however, lamellar segregates are formed as a result of the growth and coalescence of separate particles of  $\alpha'$ -phase lying in the same direction, in the same plane, without any change in the type of crystal lattice.

with the object of discovering the possibility of ~~deformation~~ <sup>formation</sup> of ~~the~~ an intermetallic compound Ni<sub>3</sub>Ti with hexagonal lattice in alloys of type KhN80T,

we ran a prolonged aging of alloy EI437 with 2.8% Ti and 0.98% Al, and also of an alloy of type EI437 with ~~added~~ <sup>additions</sup> molybdenum and tungsten (grade EI445). A study of the microstructure of the alloy <sup>of</sup> grade EI445 showed that at 700°C the diffusional processes, owing to the presence of molybdenum, are so slow that the  $\alpha'$ -phase maintains submicroscopic size for 2500 hr; its coagulation proceeds mainly along the grain boundaries (Fig.14,a). At 770°C, after holding for 1000 hr, besides the distinctly visible <sup>precipitates</sup> ~~segregations~~ of  $\alpha'$ -phase, a lamellar phase appears in the structure, mainly along the grain boundaries (Fig.14,b). An increase in the aging temperature ~~to~~ 850°C promotes the formation of the lamellar phase after holding <sup>for</sup> 500 hr. After holding <sup>for</sup> 1000 hr, at 850°C, the ~~number~~ <sup>number</sup> and size of the lamellae are very substantial (Fig.14,c).

In alloy EI437, the process of formation of a lamellar phase proceeds at lower temperatures than in alloy EI445. Such lamellar <sup>precipitates</sup> ~~segregations~~ were also observed by us ~~as well~~ after prolonged aging of alloy EI444 (type EI437 with <sup>additions</sup> of 1.5% Mo ~~added~~). Figure 15 shows a <sup>photo</sup> micrograph of the alloy after aging <sup>for</sup> 1000 hr, at 900°C. It will be seen that the growth of ~~the~~ a lamellae takes place, in accordance with the general theory of phase formation, <sup>on account of</sup> the dissolution of the neighboring particles of the  $\alpha'$ -phase and <sup>the</sup> diffusion of titanium atoms toward the growing lamellae.



c

b

a

Fig.14 - Alloy of Grade EI445 after Prolonged Aging:

(a) 2500 hrs at 700°C; (b) 1000 hrs at 770°C; (c) 1000 hr at 850°C. 600 x

The nature of the lamellar phase appearing in the alloy was determined by the electron ~~microscopy~~ <sup>diffraction method \*</sup> ~~camera~~ Polished specimens of alloys EI437 and EI445 were

etched in a special reagent in such a way that particles of ~~the segregated~~ <sup>precipitated</sup> phase stood

out above the surface of the

section. The electron-

diffraction patterns ~~microscopy~~ were taken by the

"reflection" methods. The ~~etched specimen~~ <sup>etched specimen was placed in the</sup> diffraction camera electron ~~microscope~~ in such

a way that the electron rays

slid along the surface of the

section under examination,

Fig.15 - Grade EI444 Alloy After Aging <sup>for</sup>  
1000 hrs at 900°C. 2250 x

passing through the microprojections. The interpretation of the electron diffraction patterns

~~microscopy~~ unambiguously indicated the existence in the alloy <sup>of a various phase</sup>

with a hexagonal <sup>lattice having the</sup> ~~lattice~~ with parameters  $a = 5.10 \text{ \AA}$ ;  $c = 8.31 \text{ \AA}$ ;  $c/a = 1.63$

(Fig.16,a). In the electrolytic <sup>precipitate</sup> ~~sediment~~ separated from alloy EI445, the

hexagonal phase was likewise found (Fig.16,b).

diffraction patterns

\* The electron ~~microscopy~~ were taken and interpreted by G.A.Kokorin and

S.B.Maslenkov.

Fig.16 - Electron <sup>Diffraction Patterns</sup> ~~Micrographs~~ of Specimen (a) and <sup>Precipitate</sup> ~~Sediment~~ (b)  
of Alloy EI445 after Aging 1000 hrs at 850°C

487

As already stated, ~~the stressed~~ by establishing a stressed state in the alloy the process of formation of the  $\eta$ -phase during aging may be accelerated.

Thus, after only 20 hrs

tempering at 850°C of ~~an~~ <sup>a stretched</sup>

~~stretched or compressed~~ <sup>stretched or compressed</sup> specimen

of alloy EI445, the beginning

of formation of the lamellar

$\text{Ni}_3\text{Ti}$  phase is already

distinctly visible (Fig.17).

It should be noted

that on the appearance of

Fig.17 - Alloy of Grade EI445 Aged 20 hrs  
at 850°C after Preliminary 10% <sup>Compression</sup> ~~Upsetting~~ 1300 x

the hexagonal phase we did not observe any sharp embrittlement of the alloy.

The hardness and ~~toughness~~ <sup>impact strength</sup> are practically the same <sup>for</sup> ~~as~~ an alloy in the two-phase state ( $\gamma + \alpha'$ ) and for specimens with an  $\eta$ -phase in the structure (Table 4).

Table 4

Structure and Properties of Alloy EI445 after Prolonged Aging  
(Mean Values)

Aging Temperature, °C	Holding Time, hr	Structure	Hardness		Impact Strength
			H <sub>v</sub>	R <sub>c</sub>	Toughness $\alpha_k$ , kgm/cm <sup>2</sup>

## CONCLUSIONS

- In alloys of the Ni-Ti system containing 5.4 wt.% Ti or more, on prolonged aging in the temperature interval 650 - 800°C, ~~the~~ <sup>the</sup> phase ( $\alpha'$ ) appears. Its <sup>is</sup> ~~of~~ <sup>that of</sup> composition close to the compound Ni<sub>3</sub>Ti, but <sup>it has</sup> ~~with~~ a face-centered cubic lattice. The particles of the phase in the plane of the polished section are square. With decreasing titanium content, the size and number of the particles of the

$\alpha'$ -phase decrease.

2. In the binary diagram Ni-Ti, the boundary of formation of the hexagonal phase  $\text{Ni}_3\text{Ti}$  ( $\eta$ ) at  $700^\circ\text{C}$  corresponds to 6.8 wt. %.

488

3. In two-phase alloys <sup>of</sup> the regions ( $\gamma + \eta$ ), <sup>the</sup> together with lamellar ~~segregation~~ <sup>precipitates</sup> of the interstitial compound  $\text{Ni}_3\text{Ti}$  <sup>are accompanied by</sup> a cubic  $\alpha'$ -phase ~~is present~~

for a long time (over 1500 hr at  $700^\circ\text{C}$ ). The stability of this cubic phase decreases with increasing temperature, with increasing aging time, and with increasing titanium content.

4. In Ni-Ti-Al alloys, at 1 wt. % Al, a second phase of the type  $\text{Ni}_3(\text{Ti}, \text{Al})$  appears at a lower titanium content than indicated by the phase diagram proposed by Taylor and Floyd. The alloy containing 1% Al and 5.35% Ti is of two-phase structure.

5. In alloys of type  $\text{NiAl}_3$ , the decomposition of the supersaturated solid solution takes place in two stages:

(a) <sup>precipitation</sup> ~~segregation~~ of an  $\alpha'$ -phase with a face-centered cubic lattice of the same type as the solid solution and having the parameter 3.58 kX. In its chemical composition, the  $\alpha'$ -phase is close to the compound  $\text{Ni}_3\text{Ti}$  in which some of the Ti atoms have been replaced by Al atoms;

(b) formation of the lamellar phase  $\text{Ni}_3\text{Ti}$  ( $\eta$ ) with hexagonal lattice ( $a = 5.10 \text{ \AA}$ ;  $c = 8.31 \text{ \AA}$ ;  $c/a = 1.63$ ).

6. The predominant <sup>processes</sup> ~~processes~~ in the transformation of the cubic  $\alpha'$ -phase <sup>are</sup> into the hexagonal  $\eta$ -phase ~~XXXX~~ diffusional and substitutional. For this reason, the rate of transformation depends on the aging temperature, the holding time,